



HAL
open science

Sensors integration for structural health monitoring in composite pressure vessels: A review

Bilal Meemary, Dmytro Vasiukov, Mylène Deléglise-Lagardère, Salim Chaki

► To cite this version:

Bilal Meemary, Dmytro Vasiukov, Mylène Deléglise-Lagardère, Salim Chaki. Sensors integration for structural health monitoring in composite pressure vessels: A review. *Composite Structures*, 2025, 351, pp.118546. 10.1016/j.compstruct.2024.118546 . hal-04709824

HAL Id: hal-04709824

<https://hal.science/hal-04709824v1>

Submitted on 25 Sep 2024

HAL is a multi-disciplinary open access archive for the deposit and dissemination of scientific research documents, whether they are published or not. The documents may come from teaching and research institutions in France or abroad, or from public or private research centers.

L'archive ouverte pluridisciplinaire **HAL**, est destinée au dépôt et à la diffusion de documents scientifiques de niveau recherche, publiés ou non, émanant des établissements d'enseignement et de recherche français ou étrangers, des laboratoires publics ou privés.



Distributed under a Creative Commons Attribution - NonCommercial 4.0 International License

Sensors integration for structural health monitoring in composite pressure vessels: A review

Bilal Meemary, Dmytro Vasiukov*, Mylène Deléglise-Lagardère, Salim Chaki

Center for Materials and Processes, IMT Nord Europe, Institut Mines-Télécom, Université de Lille, F-59000 Lille, France.

*Corresponding author's e-mail: dmytro.vasiukov@imt-nord-europe.fr

Abstract:

Filament-wound Composite Pressure Vessels (CPVs) are employed largely for gas or fluid storage under pressure in aerospace, automotive and naval industries. Composite vessels are subjected to harsh conditions such as critical loadings, extreme temperatures, and bursting; therefore, a permanent in-situ and online monitoring approach for the structural integrity of the vessels is essential. Hence, this review paper focuses on the description of the most trending used sensors such as piezoelectric (PZT and PVDF), piezoresistive (BP and MXene) and fiber optic (SOFO®, OBR and FBG) sensors, for developing a Structural Health Monitoring (SHM) approach to create self-sensing composite pressure vessels. The novelty of this review paper lies in providing an overview of existing works covering the integration of sensors in composite vessels, including sensor types, localization, and their impact on composite integrity. Particularly, an analysis of the literature is provided concerning the sensor's integration and especially their monitored parameters, layout design and arrangement in CPVs. Additionally, the interaction between the host composite material and sensors is analyzed to understand how to integrate sensors with the minimum possible defects that alter the mechanical performance of composite vessels. Lastly, a discussion of a CPV's SHM system is provided to offer researchers a foundation for upcoming experimental work.

Keywords: Composite pressure vessels, Filament winding process, Structural health monitoring, Embedded sensors, Composite degradation.

1- Introduction

Composite pressure vessels (CPVs) are the most advanced equipment for high-pressure liquid or gaseous fluid storage applications such as hydrogen energy, methane, and compressed natural gas (CNG) [1], [2], [3], [4], [5], [6]. These composite tanks are widely employed in various industries for transport applications such as aerospace [7], automotive, and naval [8] thanks to their high stiffness-to-weight ratio, high durability and excellent fatigue and corrosion resistances [9], [10]. Recently, the applications of CPV have been extended to hit the sanitary and heating industry for domestic hot water storage purposes [11]. CPV applications range from 10 bars for domestic uses to 700 bars for hydrogen storage applications. In general, carbon fibers (CF) are used for high-pressure storage applications, while for low-pressure storage glass fibers might be used.

Conventional CPVs consist of two main regions: a cylindrical region and two end domes on the extremity regions of the tank. The most mature and promising technology for the manufacturing of such composite vessels is the filament winding (FW) technique [12]. FW technique consists of winding continuous fibers around a rotating mandrel called a liner as shown in Fig. 1. The primary role of the composite is to ensure the load-bearing capacity of the structure, while the liner serves as a barrier to prevent gas or water leakage.

This work is licensed under the Creative Commons CC BY License. To view a copy of the license, visit <https://creativecommons.org/share-your-work/ccllicenses/>

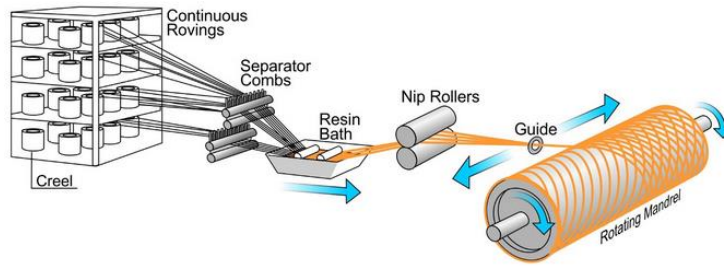


Fig. 1. Schematic representation of filament winding process for composite vessel manufacturing [13].

Three types of winding are distinguished as can be seen in Fig. 2. Firstly, hoop winding which corresponds to winding fibers with an angle of 90° with respect to the axis of the mandrel, in reality slightly less than 90° , usually 85° to 90° to allow next fiber winding circuit. The advantages of this winding are to resist the tangential forces induced by the pressure inside the tank and ensure the circumferential resistance of the structure. Secondly, helical winding consists of winding fibers with an angle of less than 90° and lies typically between 5° and 85° . The advantages of this winding are to ensure the stability of the ends of the tank and participate in carrying the axial loads. Thirdly, polar winding consists of winding fibers from pole to pole with an angle that depends on the mandrel's length. This winding is largely used for CPVs with spherical domes.

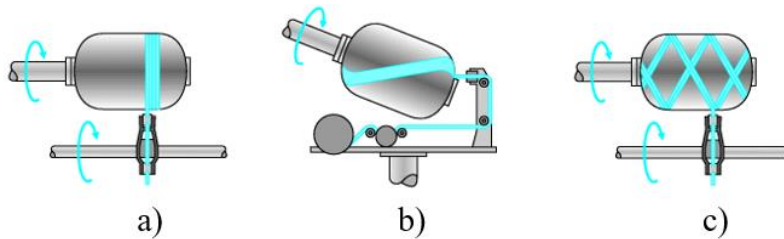


Fig. 2. Types of filament winding: (a) hoop; (b) polar; (c) helical [14].

Standard industrial pressure vessels can be categorized into five types [12], [15], [16], [17] as illustrated in Fig. 3 and have the following features: type I is a full metal vessel, type II represents a metallic liner wrapped with composite hoop layers, type III is described by a metallic liner wrapped with hoop and helical composite layers, type IV is a polymer liner wrapped with hoop and helical composite layers and type V is a liner-less tank with a full hoop and helical composite layers.

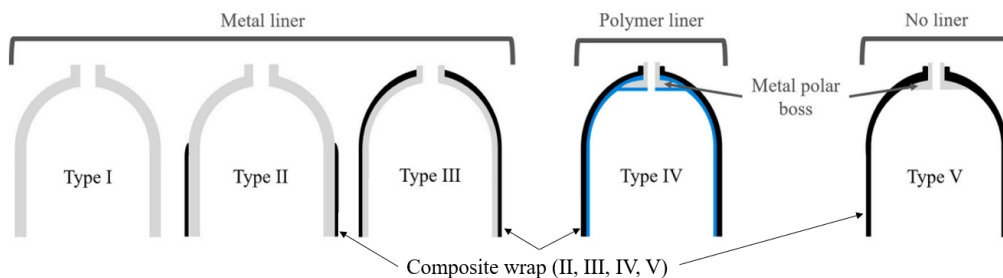


Fig. 3. Five various types of industrial pressure vessels (reproduced from [16])

CPVs offer a cost-effective solution for storing high-pressure gas and liquid across a wide range of volumes, from several liters to thousands of liters. During operation, storage tanks are subjected to the following harsh environmental and loading conditions: high temperature, internal pressure, hydrothermal aging, and cycling loading. Thus, they are classified as risk structures. Consequently, these structures may face various damage modes and failure mechanisms that might be a challenge to their structural integrity. Due to the effect of the composite material anisotropy and the possibility of unexpected damage generation, they necessitate a much deeper mechanical understanding. Therefore,

precise knowledge of the state of the tank is mandatory to guarantee safe use during its lifetime and prevent a catastrophic event; thus, the safety and reliability of the tank are of fundamental interest. This requires the development of a diagnostic and inspection technique for monitoring the state of health of the composite tank from the initial stage of damage onset.

These reasons urge researchers to improve the security of CPVs and develop a continuous, permanent, real-time and in-service structural monitoring approach for vessels that consider the local structural environment. This approach, known as Structural Health Monitoring (SHM), involves regular measurements and checks of multiple physical parameters, such as displacement and temperature, during the operation of the composite vessel through sensor integration. SHM is largely used also in other composite structures applications [18], [19], [20], [21], [22], [23], [24], [25], [26], [27], [28] like marine [29], [30], [31], aerospace [32], [33], [34], [35], civil [36] and wind turbines [37], [38], [39], [40], [41] to control and maintain good integrity of the design.

Several non-destructive evaluations (NDE) techniques are available as a sub-concept of SHM for damage detection and strain measurement analysis of CPVs such as digital image correlation (DIC) for full-field strain observation [9], [42], [43], [44], [45], [46], acoustic emission (AE) [9], [10], [47], [48], [49], [50], [51] and ultrasonic wave testing [52], [53], [54], [55]. The use of these techniques is detailed in the following standards: DIC [56], AE [57], [58] and laser ultrasonic testing [59]. However, they are employed for external and periodic assessments [4], posing challenges in implementation for high-pressure vessel testing due to limited working space [60], and are not ideally suited for long-term online monitoring during the *in-situ* operation of the CPV [61].

Fortunately, the FW technique offers the possibility of the integration of sensors during the fabrication process of CPV which is the main subject of this review. The SHM approach employed for CPVs is established by the use of a complex strategy based on wired and wireless sensors. These enable the detection, localization, identification and prediction of damage permanently and continuously. The recent analysis of the literature illustrates that the following sensors can be integrated for SHM of CPVs comprise piezoelectric sensors (PZT and PVDF) [49], [62], [63], [64], piezoresistive carbon nano-material sensors (BP and MXene) [65], [66], [67], [68], [69] and fiber optic (FO) sensors (FBG, OBR and SOFO® interferometric) [42], [70], [71], [72], [73], [74], [75], [76], [77]. To the best of our knowledge, these sensors were mainly integrated into type III and type IV CPVs.

The SHM system for CPVs will rely on sensors embedded within the composite material or mounted on the outer surface of the vessel. Embedding sensors into the bulk of the material will provide additional protection to the sensors since they are not in contact with the external environment, conversely to surface-mounted sensors. Although the SHM method for CPVs can provide significant benefits in terms of damage monitoring and detecting critical parameters, high requirements are imposed for the proper installation of such a complex system. This is mainly because embedded sensors may create discontinuities among layers, manifesting as resin-rich regions generated around sensors, which depend on the sensor's geometry, dimensions and orientation. Such resin-rich regions may impact and degrade the mechanical performance of the host composite material. These effects occur and evolve across multiple scales (micro, meso, macro) depending on the applied loading, and can prematurely lead to the failure of the CPV structure.

This review on SHM sensors for CPVs is meticulously designed to cater to a diverse audience, including novices, experts, and interdisciplinary researchers. For novices, foundational knowledge on SHM and filament-wound CPVs is provided, including detailed background information on filament winding technology, SHM principles, various sensor types, characteristics and working principles, helping them build a solid understanding of these topics. For experts, detailed analysis and recent advancements in SHM technology are offered through in-depth discussions on sensor technologies employed for monitoring CPVs, integration methodologies within filament-wound products, mechanical impacts of each sensor's type on the integrity of the host composite, and innovative research findings, along with

critical evaluations of current studies and identification of research gaps. This helps experts stay updated and aids their research and development efforts. For interdisciplinary researchers, the review connects insights across various fields related to SHM and composite materials. This work proposes a streamlined approach to better sensor selection for CPVs. Analyzing the characteristics, advantages, disadvantages, mechanical impact, applications, and degree of use of various sensor types, allows researchers and engineers to efficiently identify the most suitable option for their specific application. This comprehensive approach ensures that the review is accessible, relevant, and valuable to all readers, regardless of their expertise level.

The present paper provides a critical review of SHM sensor technology used to achieve self-sensing CPVs and analyzes their impact on the composite host material's mechanical performance. The unique contribution of this paper is its comprehensive examination of existing research on the integration of sensors within CPVs, encompassing various sensor types, their placement, and their effects on the structural integrity of the composites. The main objective of this article is to respond to the following three questions: what is the best type of sensor that might be used for CPV's monitoring? How and where should be integrated? What are their impacts on the mechanical performance of the composite? To do this, firstly a review of the principal sensor types employed for self-sensing CPVs is presented. Secondly, a state of the art regarding the integration and installation of each sensor's type in CPVs is presented. Thirdly, experimental and numerical studies about the impact of embedding sensors on composite material's properties degradation are also presented. This inspired us to discuss the best solutions for integrating sensors in CPVs (types III and IV) with minimal risk to have induced damage in a composite. Note that the solutions discussed in this review also apply to type V CPVs, as they are made from composite materials. However, they are not extensively covered here because they have not been widely studied in the literature for SHM purposes. The discussed solutions provide a foundation for constructing an SHM system, which can serve as a basis for further research.

2- Scopus metrics for sensor-enabled monitoring for CPVs

This review paper addresses a critical and rapidly evolving field within CPV technology; the integration of sensors for enhanced monitoring and safety of CPVs. The increasing complexity of CPVs has led to a growing demand for advanced monitoring solutions to ensure their reliability and safety. It is recorded a significant rise in research publications focusing on sensor integration for CPVs. The conducted analysis of publication trends using the keywords "Composite Pressure Vessel" and "Sensor" between the years 2005 and 2022 underlines this growing interest, highlighting the importance of this research field. The analysis is limited to some filters including an article document type and an English language article. The growing publication trends motivate authors to group this field of research and build a robust foundation to facilitate the development of more reliable, efficient, and safe CPVs for various industrial applications. The attached graph (see Fig. 4) illustrates a clear upward trajectory in the number of documents published on this topic, with a notable increase beginning around the year 2016 and a significant rise from 2020 onwards. This trend indicates a growing recognition of the importance of sensor integration for monitoring CPVs. Therefore, as the use of CPVs continues to expand, the importance of effective monitoring systems becomes increasingly paramount.

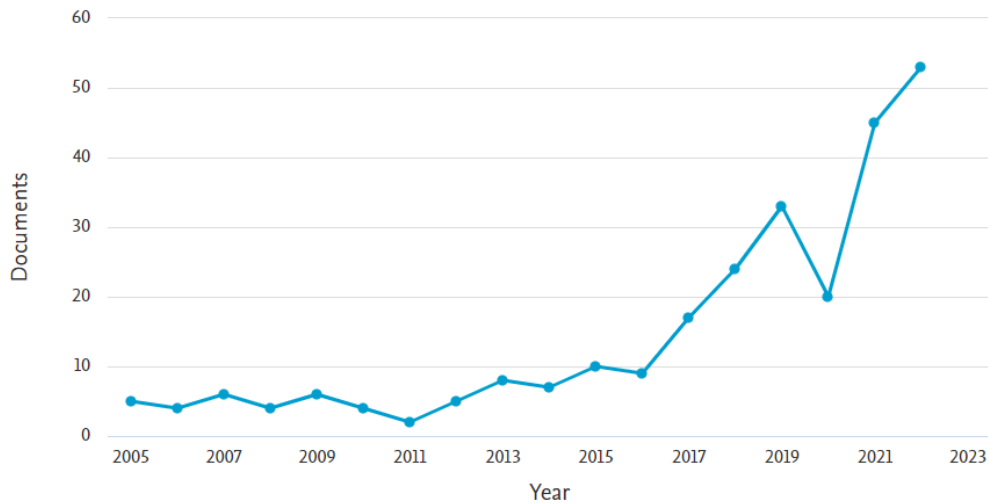


Fig. 4. Documents (publications) in the field of integrated sensors for CPV's monitoring

3- SHM sensors used for CPVs

Structural Health Monitoring represents the measurement of a structure's loading, operating environments, and critical responses to evaluate and track damage and anomalies that may affect reliability, serviceability, and safety. The main functions of the SHM system are to record the activity of a structure throughout its operation, to provide information regarding dangers that may affect the structure's performance, to enhance the real-time understanding of the CPV's behavior, and thus to improve the safety of a structure.

Sensors applied for SHM of CPVs structures require specific features, like lightweight, small dimensions, good signal-to-noise ratio, wireless construction, long service life, and low cost [78]. An SHM sensor should meet the following basic prerequisites: first, it should be independent of environmental variation and capable of monitoring the real damage of the composite material; second, it should transmit a good signal and produce as much as possible a little impact on the composite host material; and third, it should be well attached, integrated into composites and simple to handle. These sensors provide information about the stress state, deformation, and temperature of the composite, aiming at evaluating the structural integrity and safety of the CPV [79]. One of the conventional type sensors used for CPV monitoring is a strain gauge [46], [65], [85], [86], [87]. Recently, SHM approaches of CPVs include piezoelectric sensors [80], piezoresistive sensors [81], and fiber optic sensors [4], [82], [83], [84]. In this review article, we will focus only on the last three types of sensors which are the most trending ones used for SHM of CPVs.

3.1- Piezoelectric

Piezoelectric sensors are generally used for strain measurements at a micro-scale with linear behavior, and they do not require pre-amplification circuits [88]. They are capable of generating electric charge when mechanically stressed; this is called the direct piezoelectric effect, allowing materials to be qualified for sensing by estimating variations in displacement or force [89], [90]. In the same way, a piezoelectric material deforms when subjected to an electric field; this is called the indirect piezoelectric effect. This allows the piezoelectric material to function as an actuator [91]. Tuloup et al. [80] published a review paper about piezoelectric sensors used for SHM and polymer matrix composite manufacturing. The piezoelectric sensor was used by multiple authors [62], [92], [93], [94], [95], [96] for CPV health monitoring. There are several types of piezoelectric sensors for different applications, among them the Lead Zirconate Titanate (PZT) sensor and the polymer sensor Polyvinylidene Fluoride (PVDF) are used in CPVs monitoring [62], [92].

Piezoelectric sensors present high mechanical strength at a low price compared to FO sensors. Additionally, they can be mounted on the outer surface of the vessel or embedded between layers of the composite vessel to increase sensor durability and ensure higher sensitivity to structural deterioration. They also offer a high electromechanical response. However, under static conditions, piezoelectric sensors may not generate a significant voltage signal. Therefore, it is important to note that they are used mainly in dynamic conditions to execute measurements and they operate for a large range of frequencies. Besides that, they are sensitive to high temperatures, which reduces their sensitivities [94]. One significant disadvantage of piezoelectric sensors is that they have a form much more complex than FO sensors. In general, they are found in circular pellet form in the market. Their diameters vary generally between 3 and 50 mm and a thickness of 0.5 mm approximately. A scheme of the piezoelectric sensor is shown in Fig. 5.

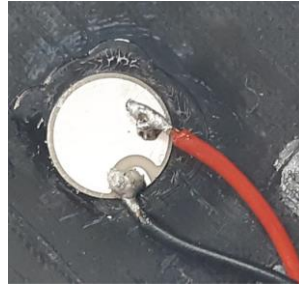


Fig. 5. Piezoelectric sensor

A network of PZT sensors covering a vast area of a structural element necessitates long and heavy cabling, which may be detrimental to the structure's performance. Three ways may be used to shorten the lead wires of a PZT sensor's network. To construct a single continuous sensor, PZT sensors in the same row or column can be linked in series, parallel, or heterogeneously, with a combination of in-series and parallel connections. These solutions allowed for shorter cabling lengths than each sensor had its lead wire attached to a single channel of the monitoring system. These strategies were validated on a composite wing of an aeronautical application [97]. The detection approach used for actuating the PZT transducers under an electric field is an electro-mechanical impedance (EMI) [98]. Typically, the real part of impedance may be used to identify damage, whereas the imaginary part of impedance can be utilized to detect transducer debonding [99]. The impedance depends not only on the thickness, length, and width of the PZT sensor but also on the mass, stiffness, and damping of the composite host structure. The changes in the impedance of the PZT sensor $Z_E(\omega)$ allow the sensing of a damage in the structure. The measurement of the impedance can be done using an impedance analyser or LCR meters (inductance L, capacitance C and resistance R). The EMI technique uses a sinusoidal source V_X , a high frequency excitation of the structure (≥ 30 kHz) and an angular frequency ω , in order to produce a current I . The electrical impedance of the PZT transducer is calculated by the following equation [100]:

$$Z_E(\omega) = \frac{V_X}{I} = \frac{1}{j\omega a} \left(\bar{\epsilon}_{33}^T - \frac{Z(\omega)}{Z(\omega) + Z_a(\omega)} d_{3x}^2 \hat{y}_{xx}^E \right)^{-1}, \quad (1)$$

where $Z_a(\omega)$ and $Z(\omega)$ represent the mechanical impedances of the sensor and monitored structure, respectively, \hat{y}_{xx}^E the Young's modulus, $\bar{\epsilon}_{33}^T$ the dielectric constant, j the imaginary unit, d_{3x}^2 the electric field constant and a the geometric constant.

Two decades ago, another supple sensor named Stanford Multi-Actuator Receiver Transduction (SMART Layer™) delivered by Acellent Technologies [101] was created to successfully attach a PZT network of sensors to structures. It represents a flexible dielectric layer device that can be integrated among composite layers of the vessel during the filament winding process as an extra ply or surface-mounted on the outermost layer of the vessel [102]. It's applicable also for both composite and metallic

structures. An epoxy adhesive bonded on one side of the SMART layer is present to achieve a good bonding with a contact surface. A technique for creating a 3D complex shape of SMART layer that maintains its shape; is to use mechanical locks at pre-chosen sites and after that form the layer on the geometry. The layer will maintain its shape after curing. A representation of this idea is shown in Fig. 6.

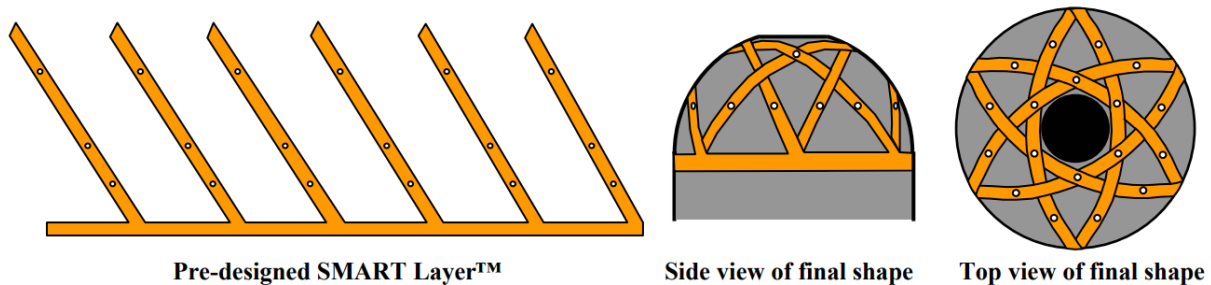


Fig. 6. Illustration of 3d SMART layer shaping on composite vessel structure [102].

The smart layer offers several advantages thanks to its small thickness, remain flexible during a high number of cycles in fatigue, durable, ease of handling, and a size of a few centimeters to a few meters [102], [103]. It demonstrates also its capability to not degrade the integrity and the mechanical properties of the composite host material [102], [104]. This is also true for showing environmental and hydrothermal aging and providing real-time analysis of data in the embedment process during the filament winding [102]. Moreover, it can support a high temperature of the order of 200°C. The SMART layer was proved to be adaptable for damage localization and detection in filament-wound CPVs [63].

3.2- Piezoresistive

In the past five years, the use of piezoresistive sensors in the field of filament-wound CPVs has increased. When sensors based on piezoresistive material are subjected to mechanical strain or stress, they respond with a change in the electrical resistance manipulated by nanocarbon materials such as polymer fillers [105], [106]. The principle of this method is that when the conductive network of sensors breaks up due to damage, the resistance of sensors in composites changes [107]. Several materials with good electrical conductivity like carbon nanotubes (CNTs) [108], [109] and graphene nanoplatelets (GnPs) [110], [111] are introduced into the nonconductive matrix to create a conductive network inside it to obtain a strain sensor applied for SHM. In other words, spreading CNTs and GnPs into a polymer to constitute a conductive matrix [112].

Embedding nanomaterial-based sensors in filament-wound CPVs for structural health monitored in situ to obtain damage information has been employed by several authors [65], [66], [67], [68], [81], [113], [114], [115]. Nauman [116] has published a review paper to present the different approaches to using piezoresistive sensing techniques for the health monitoring of polymer composites. Lemartinel et al. [117] have published a review paper that presents nanocarbon-based materials sensitive to strain and damage for SHM of composite parts. Nanocarbon materials can also provide a reinforcing effect by enhancing the mechanical properties of the composite structures. While carbon fiber can be self-sensing, it can be used to introduce nanocarbon materials into fiber-reinforced polymer (FRP) composites to take advantage of their piezoresistive properties for sensing purposes. In the case of using carbon fiber for CPV, this might be used as a self-sensing strategy by making their sensors for damage monitoring [32]. This method helps for avoiding the introduction of sensors in the CPV fabricated by carbon fiber, to prevent the impairment of the mechanical properties of the composite materials. CNTs offer great advantages such as they have great mechanical strength and high thermal and electrical conductivities [118], [119]. In addition, CNTs can be assembled easily into the nonconductive polymer matrix to form networks that possess electrical conductivity. There are two applications of CNT-based sensors in CPV: buckypaper (BP) sensors [65], [66], [68], [113] and MXene sensors [66], [67], [68], [115]. The in-situ

monitoring of the strain values for both types of sensors is conducted with the knowledge of the relative resistance $\Delta R/R_0$. The increase of the resistance measured by these sensors implies that a structure's deformation occurs. Thus, this parameter is normally used to describe the sensitivity of these sensors. The resistance of these sensors can be recorded by the FLUKE 2638A counter as mentioned in [65], [67]. The relative resistance is calculated by the following equation [113].

$$\Delta R/R_0 = \frac{R-R_0}{R_0} \times 100\%, \quad (2)$$

where R is the test resistance during loading and R_0 is the initial resistance before the mechanical loading.

The BP sensor consists of the dispersed CNTs in a solvent solution which are then filtrated through a polymeric membrane to fabricate a film [65]. The preparation method of the BP sensor is introduced in [65], [120], [121]. They used commercial multi-walled carbon nanotubes (MWCNTs) with a length and diameter in a range of 30 to 50 nm and 10 to 12 nm, respectively. BP sensor is a three-dimensional (3D) mesh composed of continuous highly entangled CNTs networks connected by Van Der Waals interactions. BP sensor has several advantages such as high reliability and sensitivity, resistance to shock, good stability, lightweight [122], and can be used in places with high curvature. Generally, the BP sensor has a circular shape illustrated in Fig. 7, but it can be changed according to the desired shape of the designer.

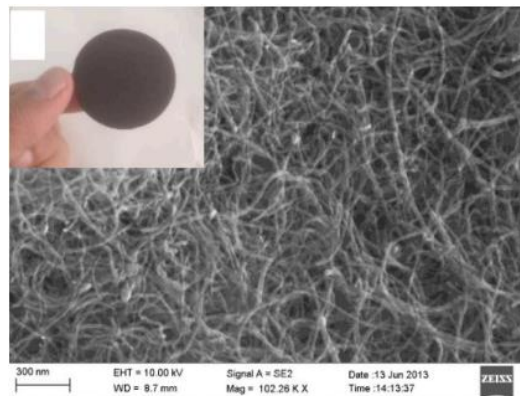


Fig. 7. Scanning electron microscopy of BP sensor [66].

The reason that the sensitivity of the BP is not very high, this fact motivates researchers to find a highly sensitive sensor [66]. Researchers have been encouraged to explore MXene Two-dimension (2D) materials sensors [123] for SHM purposes thanks to their excellent mechanical properties and high conductivity. MXene possesses a conductivity of $2.4 \times 10^5 S/m$ which is more significant than other nanomaterials like CNT around $400 S/cm$ [67]. The definition of MXene consists of “M” which represents metal and “X” which is nitrogen or carbon [124]. The piezoresistive response of MXene sensors is described by its sensitivity and characterized by the rate of resistance change $\Delta R/R_0$.

The structure of the MXene sensor consists of a layered form, so it allows the fabrication of a sufficiently sensitive pressure sensor with a high compressive property. The preparation and fabrication method of the MXene sensor is reported in the references [67], [115], [125]. MXene sensors are made generally on a flexible printed circuit (FPC) from which the embedment sensors are linked to the data acquisition system. The role of the FPC is to avoid a short circuit between the conductive carbon fibers and the metallic wires, survive the sensors, and enhance their stability. The FPC thickness is just 0.1 mm, hence it may decrease the impact defects due to the embedment of the conductive wires. Moreover, a silver paste that represents a bonding material, is employed to bond sensors and electrodes together on the FPC. This bonding material helps with contact resistance minimizing at the MXene-electrode interface [67]. In Fig. 8, we represent four circular shapes of MXene sensors applied on an FPC.

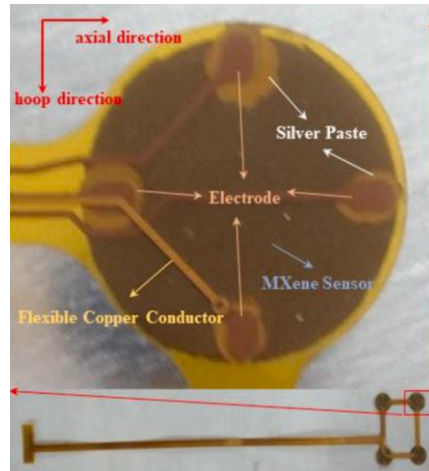


Fig. 8. MXene sensors details made on FPC [67].

3.3- Fiber optic sensors

Fiber optic (FO) sensors are employed for tracking and monitoring various parameters required to evaluate the health state of composite structures, especially CPVs. Their primary role is to detect damage that causes a variation in stiffness, which can be indicated by fiber optic's changes in their optical properties, for instance, wavelength, intensity, and polarization [126], [127]. FO sensors are receiving increasing attention compared to other types of sensors thanks to their crucial advantages such as a simple way of integration with composite material, small dimension, lightweight, high sensitivity and continuous monitoring in the long term period, durability, resistance to electromagnetic interference and authorize multiplexing sensors in the same FO sensor [33], [128]. The fundamental reason to integrate a FO sensor is that the sensor itself is a fiber that can mix with other fibers of a composite. Nevertheless, FO sensors are very expensive compared to other types of sensors because of the optical processing signals and electronic systems. Due to the sensitivity of FO sensor to moisture and chemical environment, it needs to be protected by a polymeric film, which enlarges the outer diameter of FO to reach more than ten times the average diameter of reinforcing E-glass or carbon fiber [129], [130]. In the next section, we discuss the different types of FO sensors used especially in CPVs for monitoring strain, temperature, and pressurization state. FO sensors applied for this purpose are categorized into three types: interferometric FO (SOFO®) sensors, distributed FO sensors by OBR technology, and Fiber Bragg Grating (FBG) sensors.

3.3.1- Interferometric fiber optic (SOFO®)

To the best of the author's knowledge, FO sensors such as interferometric sensors: (SOFO®) or Fabry-Perot (F-P) are less frequently employed for composite vessel monitoring [74], [131], [132]. Interferometric sensors carry a single-point detection. Thus, it is hard and difficult to render them multiplexed. The principle work of an interferometric sensor is based on an extrinsic or intrinsic cavity located along the fiber, when physical modifications happen to the host structure, it reflects a different optical phase between two interference light waves [133]. Fabry-Perot sensors can operate at a range of temperatures from -40 to $+250$ °C. Add to this also that they are characterized by their high strain resolution of around $0.15 \mu\epsilon$ with a range of strain measurement of $\pm 5000 \mu\epsilon$. The whole system is constituted of software analysis, sensors, data acquisition, and a reading unit. The standard SOFO sensor consists of two fiber optics called the reference fiber and the measurement one, and they are contained in the same protection tube. The measurement fiber is connected to the host structure and tracks the structure's changes. The reference fiber is independent of the structure's deformations. The reading unit sends the optical signal, or light, through a coupler to the sensor. The light reflects off by mirrors positioned at the ends of each fiber and returns to the reading unit to be demodulated by a pair of matching fibers. The information on the structure's deformations included in the returning light is

decoded in the reading unit and displayed on a portable PC [74]. The setup and components of the SOFO interferometric sensor system are shown in Fig. 9.

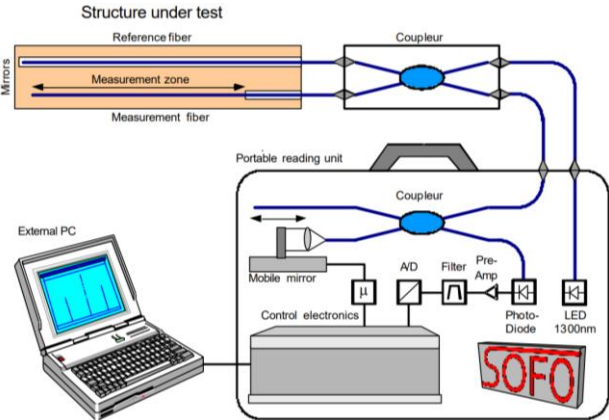


Fig. 9. Setup and components of SOFO interferometric sensor system [134].

3.3.2- Distributed fiber optic by OBR technology

The Optical Backscatter Reflectometry (OBR) technology was first implemented by Maurin et al. and Klute et al. [135], [136] in the monitoring of CPVs applications. Then, OBR distributed optic fiber sensor was used by Saeter et al., Munzke et al., Souza et Tarpani, Liang et al., and Shamsuddoha et al. [70], [72], [73], [137], [138] in CPV applications. The OBR is an instrument based on Rayleigh backscattering. They are apt to deliver a continuously measured profile at any location along the length of the fiber. Aiming at performing and providing a full-field measurement of strain and temperature over large structures like pipelines and aircraft. Add to this, that this technology of FO permits measuring strain with a resolution of millimeter range along large distances (up to 70 m) [72], [130].

Generally, an OBR fiber optic sensor has respectively the diameters of the fiber core, cladding, and polymer coating of $d = 6.5 \mu m$, $D = 125 \mu m$ and $\phi = 155 \mu m$ (see Fig. 10).

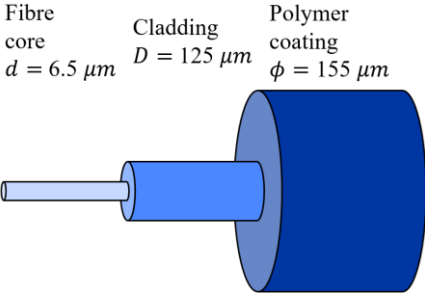


Fig. 10. Fiber optic constituents schematization.

The Primary Coated Fiber optic (PCOF) characterized by the measuring fiber, is embedded typically in the composite layup. The PCOF is spliced to a robust Secondary Coated Fiber optic (SCOF), which has the function of transferring the signal to the outside of the composite tank. In addition, SCOF possesses a connector port to the LUNA OBR 4600 Apparatus. Luna Innovations [139] is one of the supplier companies of the OBR apparatus and its software. An explicit description of how to measure the change of the strain field among composites and the distributed fiber optic sensor OBR is assigned in the paper of Grave et al. [140]. The OBR fiber optic and its interrogator are shown in Fig. 11.

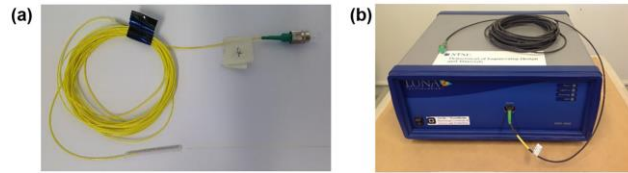


Fig. 11. OBR sensor and its interrogator for distributed strain measurement: (a) SCOF with a connector and a tag. (b) Luna OBR 4600 interrogator [72].

3.3.3- Fiber Bragg Grating (FBG)

FBG sensor represents the most common FO sensor applied for measuring the change of strain (displacement) and temperature in CPVs application [4], [60], [61], [70], [75], [92], [131], [132], [135], [141], [142], [143], [144], [145]. It is composed of a silica-based core, surrounded by a silica cladding and protected from the outside by a polymer coating [32]. A light wave enters the FBG which reflects the incident light with a specific wavelength and the rest of the spectrum is transmitted. When there is a variation in temperature or axial deformation, the reflective Bragg wave λ_B will shift steadily, resulting from the changes in fiber size (stretch, compression) and thermal effect [146]. The concept of FBG detection is that the deformation $\Delta \epsilon$ of the CPV is figured out from the offset of the wavelength [147]. A typical schematic diagram for FBG monitoring of CPV is illustrated in Fig. 12.

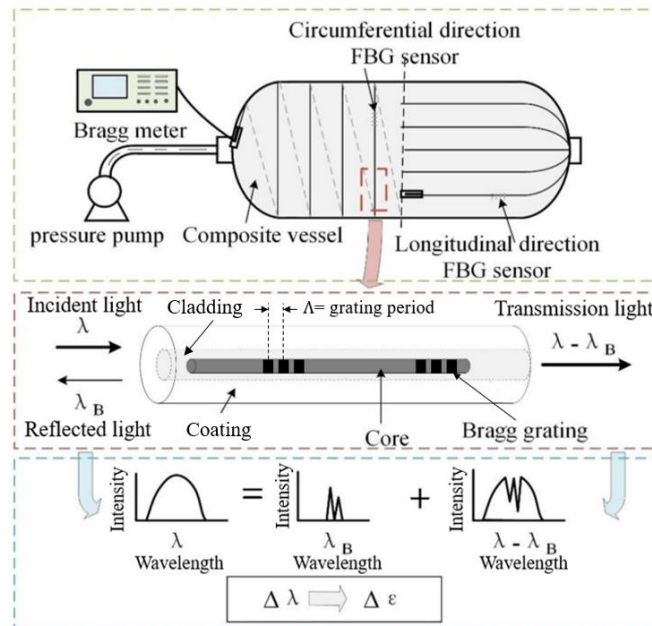


Fig. 12. Representation of FBG sensor for CPV [147].

FBG sensors have interesting advantages: their capability to detect and perform local measuring in real-time on the tank either under dynamic or static deformation. Not like SOFO sensors, FBG sensors have the capability of multiplexing, it's feasible to incorporate many FBGs to create a network of sensors (named quasi-distributed systems), so that is essential when having a complex system of SHM [61]. In other words, this technique allows to realize several measurements in the same sensor. This feature allows monitoring the whole vessel structure with less wiring, maintaining a lightweight structure as compared to piezoelectric and strain gauge sensors [33], [128]. This type of sensor allows local measurements of temperature and strain over enormous areas and at specifically required zones. Moreover, it presents a small size (fiber core diameter $d = 10 \mu m$, cladding diameter $D = 125 \mu m$, polymer coating diameter $\phi = 250 \mu m$). Furthermore, it is lightweight, durable, immune to electromagnetic interference and a long-term high sensitivity [61], [92]. The FBG sensor can be used in many applications such as strain and temperature measurements, resin cure monitoring, process

monitoring, and localization of damage [32]. FBG sensors offer higher precision and accuracy in measuring strain, temperature, and other parameters due to their localized measurement capability, while OBR sensors provide distributed measurements along the entire length of the FO.

FBG sensors are characterized by the Bragg law equation, where the reflected Bragg wavelength depends on the Bragg grating period Λ (represented in Fig. 12) and the effective refractive index, following equation [33]:

$$\lambda_B = 2\eta_{eff} \Lambda \quad (3)$$

The presence of local deformation yields grating period variation and modifies the reflected wavelength consequently, resulting in a local strain according to the following equation [33]:

$$\frac{\Delta\lambda_B}{\lambda_B} = (1 - \rho_e)\varepsilon, \quad (4)$$

where ρ_e is the photo-elastic coefficient of the fiber core material with a value of $\rho_e = 0.22$ in the case of silica core fiber, and ε represents the longitudinal strain.

4- Sensors integration in CPVs

The integration of sensors in CPV may be embedded between composite layers or surfaces mounted on the external layer of the tank [32]. Embedding systems of sensors offer the possibility of efficient detection of critical parameters for example strain and temperature variation. Besides, it provides extra protection from the surrounding environment which improves the sensor sensing accuracy, and enhance potentially its durability and lifetime [148], [149]. Moreover, embedding sensing systems allows for sensors to have high sensitivity, stability, and durability [34]. However, this system may face a high temperature, that may harm the sensor [30], [150], [151], [152], [153], [154], [155]. Ren et al. [155] studied the temperature effects on embedded PZT signals in SHM for composite structures. The findings reveal that the signals decrease with increasing temperature from -50 to 70°C. Mahmood et al. [153] have analyzed the temperature-dependent strain and damage monitoring of glass fiber/epoxy composites with piezoresistive sensor. They found that the electrical resistivity reduces by approximately 30% when increasing temperature from zero to 50°C. Kressel et al. [150] have evaluated the temperature effects on the FBG reading. They concluded that the grating period and the FBG refractive index depend on the temperature. Moreover, the embedment of a high quantity of sensors may degrade the mechanical properties of the host composite. In the case of embedded sensors for CPV application, they can be located directly on the liner and/or among composite plies. According to numerical studies and hydraulic tests, these represent the zones that are the most stressed in the entire vessel. On the flip side, surface-mounted sensors are more practical from the implementation point of view, maintenance, and replacement. It has little effect on material degradation compared with the embedment of sensors between layers. However, surface-mounted sensors without extra protection may be damaged by external impact [149]. The use of a sensing system offers a definite substitute for the current non-destructive evaluation techniques because it cannot be used for continuous monitoring of vessels.

SHM technology is still in development and faces major challenges. To detect damage accurately, not only an adequate mechanical bonding connection must be presented between the integrated sensor and the host composite structure but also an adequate placement of the sensor not far from the critical area is needed for better monitoring. In this way, the sensor is then subjected to the same strain variations as the host structure. The most appropriate method for choosing the location of sensors is to numerically model and study the vessel based on the finite element method (FEM). Thanks to this modeling technique, stress concentration appears on a localized zone in the vessel, whether in the dome, cylindrical, or/and on the junction between the dome and cylindrical part. Once the stressed zones have been known, in this way the number and position of sensors can be determined.

The embedment strategy of piezoelectric, piezoresistive, and fiber optic sensors into the vessel layup consists of the following steps: 1) initiation of the filament winding; 2) pausing the filament winding at the predefined level; 3) positioning sensors between two layers at their designated locations; and 4) resuming the filament winding.

In this section, a comprehensive analysis of the sensors' integration in filament-wound CPVs is explored in a table form. Each table summarizes critical aspects for each type of sensor, including a chronological sequence, CPV's type and material, monitored and controlled parameters, sensor layout design and arrangement in CPVs, loading type, and principal conclusions. This structured format allows for a clear and organized presentation of data, facilitating easier comparison and understanding of the various methodologies employed.

In the following, an analysis of the integration of piezoelectric, piezoresistive, and fiber optic sensors in CPVs is provided through both qualitative and quantitative approaches. Table 1, Table 2, and Table 3 provide detailed schematics of sensor placement and quantity in composite vessels, offering a clear view of the integration process. The qualitative analysis addresses clarity, precision, vessel shape, materials, sensor types, and notations, while the quantitative analysis focuses on the number of sensors, accuracy of numerical values, and sensor placement distances. This approach ensures a comprehensive understanding of the methods and results, highlighting the methodologies of developing an effective SHM system.

4.1- Piezoelectric

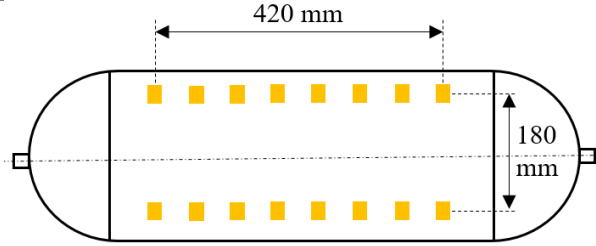
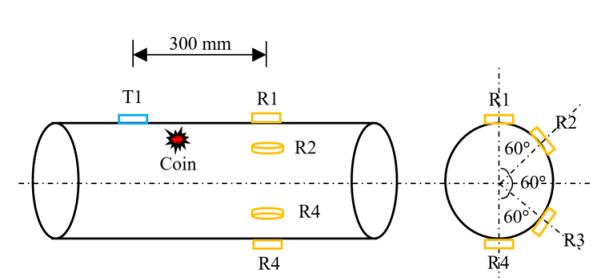
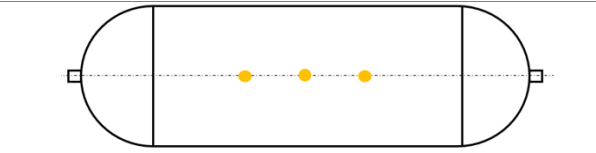
Herein, the integration of piezoelectric sensors in CPVs is analyzed in some punctual years as found in the literature. This analysis offers an overview of embedded or surface-mounted piezoelectric sensors in mainly type III CPVs and composite tubes. This type of sensor is used primarily for strain monitoring and damage detection during cyclic pressure loading or impact tests.

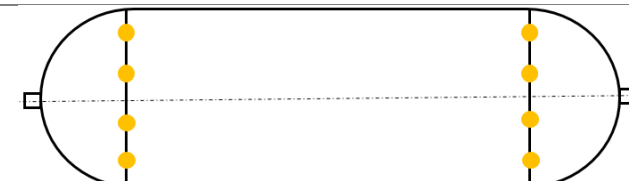
Several studies [63], [92], [64], [62], [156], [96] have explored different approaches for detecting and localizing damage in CPVs using piezoelectric sensors. A study [63] involved embedding SMART Layers™ PZT network sensors into a composite bottle during the filament winding process, showcasing their potential for damage localization through sensor signals in a specific frequency range. The use of SMART Layer™ PZT attach network sensors has not been implemented since several years ago. Additionally, PVDF and FBG sensors were embedded in a common type III CPV to compare their sensitivity, with PVDF sensors proving effective for dynamic measurements [92]. Another study [62] focused on bonding PZT sensors on the outer surface of a composite pipe, demonstrating their reliability for detecting and locating defects like delamination. This study has been investigated via a coin placement among sensors that results nonlinearities in the propagation of waves. However, from the author's point of view, the technique's reliance on a coin for inducing nonlinearity raises concerns about its practical applicability in a real-world scenario. Another novel approach employed guided ultrasonic waves and PZT disk sensors to accurately localize damage under high frequency conditions. This study demonstrated the effectiveness of PZT sensors in accurately localizing damage under high-frequencies.

Overall, while these studies contribute to advancing SHM technologies in CPVs applications, there is a need for comprehensive evaluations to address practical challenges and ensure the reliability of these sensor systems in real-world conditions. The studies conducted above provide valuable insights into the use of various sensor technologies for damage detection in CPVs. The detailed studies in the literature concerning the piezoelectric sensor integration in CPVs are summarized in Table 1, chronologically.

Table 1. Piezoelectric sensor integration in CPVs

Year	CPV's type and materials	Monitored and controlled parameters	Piezoelectric sensors layout design and arrangement in CPV	Loading type	Principal conclusions	[Ref]
2006	Type III Liner: aluminium Composite overwrap: carbon fiber layers.	Damage detection.	<p>● 5 PZT sensors in each smart layer strip ■ 8 spaced strips containing 5 PZT sensors: Total 40 PZT sensors in the bottle</p> <p>2 helical plies Total 5 hoop plies Smart layers</p> <p>Aluminum</p>	Impact test.	<p>SMART layers can be integrated during the filament winding process.</p> <p>The range of frequency 35-65 kHz was the best interval to detect damage to the bottle through sensor signals.</p>	[63]
2010	Type III Liner: steel Composite overwrap: glass fiber-polypropylene.	Strain monitoring during operational service.	<p>— FBG in hoop direction — FBG in axial direction</p> <p>■ Two PVDF sensors placed symmetrically with respect to the vessel axis Sensors are located on the interface liner-composite overwrap</p>	Cyclic internal pressure loading.	<p>FBG fiber optic presents an alternative solution tool when comparing it with piezoelectric sensors.</p> <p>In the case of dynamic measurement PVDF sensor technology proved that it was an effective tool and it had a good resolution.</p>	[92]

2016	Type III Liner: aluminium Composite: carbon fiber reinforced polymer.	Impact damage detection et localization (delamination and disbonds) using guided Lamb wave.	 <p>Two arrays of PVDF sensors, each containing 8 sensors Sensors bonded on the outer surface</p>	Impact test.	PVDF is a reliable bonded transducer because they are light and flexible to bond on curved profiles.	[64]
2021	Composite pipe Composite overwrap: glass fiber layers.	Damage detection (delamination) due to nonlinearities of guided wave between transmitter (T) and receiver (R) sensors.	 <p>PZT sensors arrangement over the outer surface of the pipe</p>	Impact test.	PZT sensors were a reliable tool for damage detection and localization of the source of nonlinearity.	[62]
2022	Type III Liner: aluminium Composite overwrap: carbon fiber with epoxy [90 ₂ /±11/90 ₂ /±11/90 ₂ /±11/±11/70 ₂]	Damage assessment by strain variation.	 <p>● PZT sensors</p> <p>Three PZT sensors (10 mm diameter and 0.25 mm thickness) bonded on the surface of the vessel</p>	Low-velocity impact test.	The localization of damage was achieved accurately using PZT sensors under high-frequency.	[156]

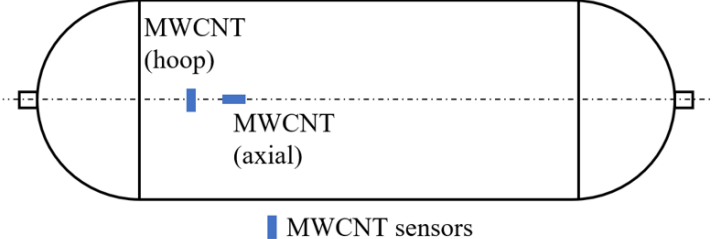
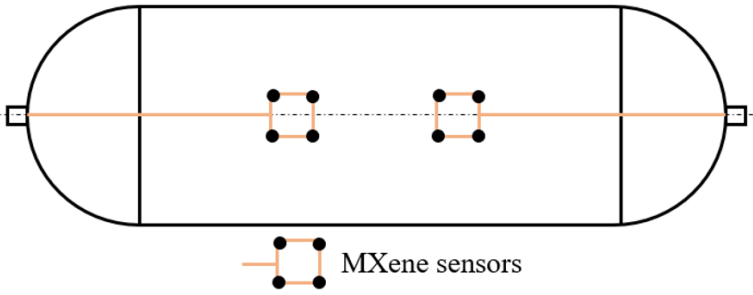
2023	Type III Liner: aluminium Composite overwrap: carbon fiber wraps with outermost glass fiber layers for a protective barrier.	Damage impact localization.	 <p data-bbox="918 375 1276 582">● Sensor array consisting of 16 PZTs, uniformly distributed at both ends of the cylindrical region No information about the integration locations</p>	Impact test.	PZT sensors can be used for damage localization accurately. [96]
------	--	-----------------------------------	--	-----------------	--

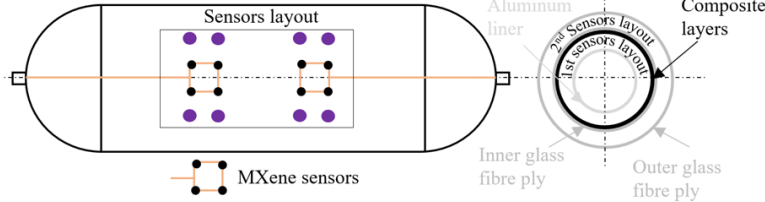
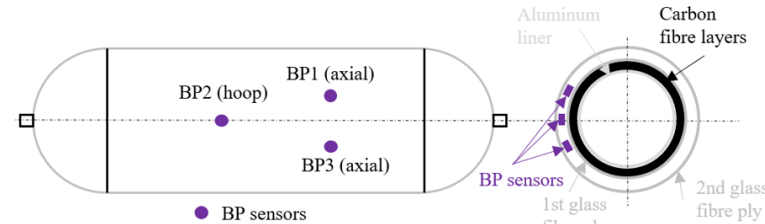
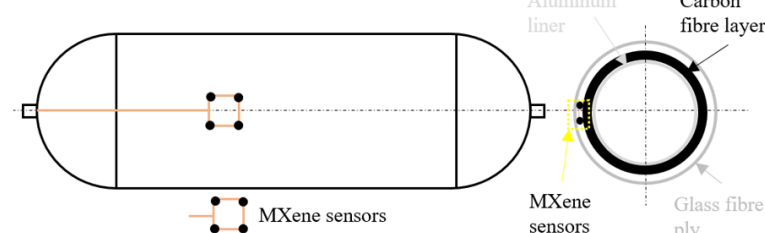
4.2- Piezoresistive

Here, the integration of piezoresistive sensors into CPVs over the past five years as documented in the literature is examined. This review provides a summary of piezoresistive sensors embedded between composite layers or mounted at the interface liner-composite, typically in only type III CPVs. These sensors are predominantly used for the detection of vessel bursting, thermal and mechanical strain monitoring, damage detection, and localization.

Recently, several authors [113], [67], [66], [65], [115], [68] based mainly in China worked only on the SHM of type III CPVs through the integration of piezoresistive sensors. By embedding various types of sensors into the vessel structure, such as MWCNT, MXene, and BP sensors, these studies have explored novel approaches for in-situ structural monitoring of CPVs. Each study presents unique insights into sensor integration, sensor orientation, and sensor performance evaluation under different loading conditions. One such approach [113] by researchers involved embedding MWCNT sensors within the composite layers, demonstrating their effectiveness in detecting burst actions and correlating signals with vessel behavior. Additionally, integration of MXene sensors onto CPVs [67] has shown promise, particularly in fatigue resistance testing where MXene sensors exhibited a regular piezoresistive response and good correlation between resistance changes and applied pressure. Further investigation [66] compared the performance of piezoresistive sensors, such as BP and MXene sensors, revealing differences in sensitivity to microcrack initiation and propagation. Additionally, the integration of BP sensors [65] proved valuable for permanent damage monitoring, showcasing their reliability and sensitivity compared to traditional strain gauges. Moreover, the use of MXene sensor arrays [115] for impact behaviour studies demonstrated their extreme sensitivity to low-energy impacts, offering efficient real-time SHM capabilities. Combining BP and MXene sensors on FPCs [68] presents a novel approach for monitoring elastic and plastic deformation, as well as thermal strain. Overall, while these studies present innovative approaches for CPV's SHM, continued research efforts are essential to address technical challenges and monitoring of a type IV and a type V CPV through these piezoresistive sensors. The aforementioned references for piezoresistive sensors integration in CPVs are all detailed and summarized in Table 2, in a chronological way.

Table 2. Piezoresistive sensors integration in CPVs

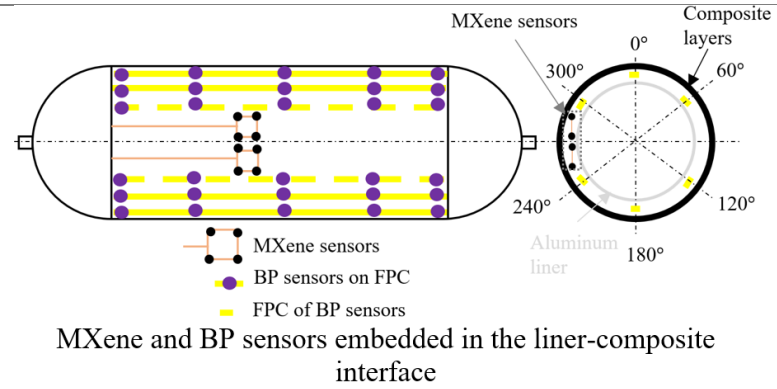
Year	CPV's type and materials	Monitored and controlled parameters	Piezoresistive sensors layout design and arrangement in CPV	Loading type	Principal conclusions	[Ref]
2019	Type III Liner: steel Composite overwrap: glass fiber-epoxy layers Stacking sequence: [90° ₁₀ / (±15°) ₂₀ / 90° ₁₀]	Detection of the vessel's bursting, changes in electrical resistance of sensors, and strain monitoring.	 <p>MWCNT (hoop) MWCNT (axial)</p> <p>■ MWCNT sensors</p> <p>MWCNT sensors embedded in the middle thickness of the composite layers</p>	Hydraulic cyclic test.	MWCNT sensor's measured signal corresponds to the mechanical behavior of the composite vessel.	[113]
2021	Type III Liner: aluminium Composite overwrap: carbon fiber-epoxy followed by two glass fiber layers for protection purposes.	Record changes in the hoop and axial strain field.	 <p>■ MXene sensors</p> <p>Two MXene sensors installed between the last two glass fibre layers on COPV</p>	Hydraulic fatigue test.	The piezoresistive sensor in the hoop direction was less sensitive than the axial direction.	[67]
2021	Type III Liner: aluminium Composite overwrap: carbon.fiber	Measurement of the changes in resistance ($\Delta R/R_0$) due to the pressure of the vessel.		Hydrostatic fatigue cyclic test.	BP sensor is more responsive than MXene sensor to the onset and propagation of microcracks in the	[66]

<p>-epoxy followed by two glass fiber hoop layers.</p>	 <p>MXene and BP sensors layout embedded in two regions: 1- on the liner-composite interface and 2- between the second and outer glass fibre layers</p>	<p>composite part of the vessel.</p> <p>MXene is more sensitive to the compressive residual strains or plastic deformation of the aluminium liner.</p>
<p>2022 Type III Liner: aluminium Composite overwrap: carbon fiber-epoxy followed by glass fiber layers for protection purposes</p>	<p>Permanently monitoring damage.</p>  <p>BP sensors arrangement between the first and second glass fibre layers in COPV</p>	<p>Fatigue and hydrostatic pressure test.</p> <p>BP sensors are more reliable and sensitive to microcrack initiation and propagation than strain gauges.</p> <p>[65]</p>
<p>2022 Type III Liner: aluminium Composite overwrap: carbon fiber-epoxy followed by glass fiber unidirectional prepreg.</p>	<p>Monitoring the position and the damage degree caused by low-velocity impact.</p>  <p>MXene sensor layout located between glass and carbon fibre layers of the vessel</p>	<p>Impact test.</p> <p>MXene sensor was extremely sensitive to low energy impact.</p> <p>The sensor was able to determine the position and location of the impact point as well as the magnitude of the energy's impact.</p> <p>[115]</p>

2022

Type III
Liner:
aluminium
Composite
overwrap:
carbon fiber
layers.

Thermal strain,
and elastic and
plastic
deformation
monitoring.



Hydraulic
pressure
cycling.

The combination of
MXene and BP sensors on
FPC could be utilized as
temperature sensors for
materials and sensitive
strain sensors

[68]

MXene sensor could
perform multi-directional
strain monitoring more
accurately than the BP
sensor.

4.3- Fiber optic

In this section, an investigation of the integration of various FO (SOFO, OBR, and FBG) sensors in CPVs as reported in the literature over certain years. This examination outlines the locations and number of either embedded or surface-mounted FO sensors in various types of CPVs and composite pipes. FO sensors are essential for monitoring during the manufacturing and lifetime operation. They can measure strain, temperature, pressurization, and process-controlled parameters (fiber tension, resin polymerization temperature, ...), and detect and localize damage.

SOFO sensors have been used in type III [131], [132] and type IV [74] CPVs. Although interferometric SOFO sensors have been used for the monitoring of CPVs, their usage remains relatively rare compared to other fiber optic sensor types. SOFO sensors were embedded sometimes alongside FBG sensors to assess structural integrity during operational service. Despite their potential, SOFO sensors demonstrated limitations in defect sensitivity compared to FBG sensors in static and cyclic loading tests. This raises questions about the effectiveness of SOFO sensors for comprehensive SHM in CPVs, indicating the need for further investigation into their practical utility and reliability. As mentioned earlier, one of the biggest drawbacks of SOFO sensors is that it is a point-wise sensors that conduct only local measurements.

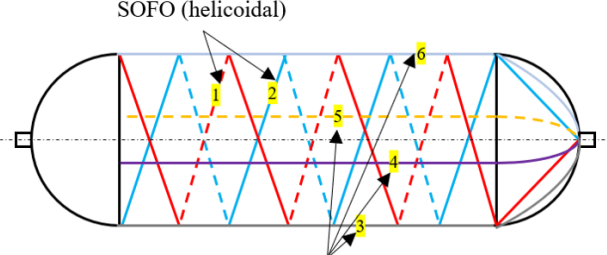
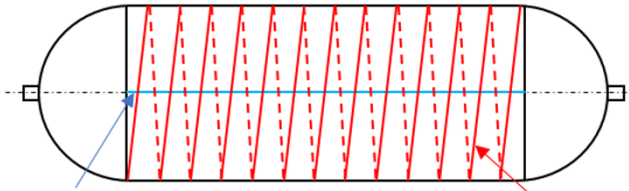
Various studies have investigated the integration of OBR optical sensors in CPVs for strain and damage monitoring. In the recent ten years, OBR sensors have been utilized across different types of CPVs starting from composite pipes [137], [157], types III [72], [136] and IV [73], [135], [138], [158] until type V [70] CPVs in the last period. Their use demonstrates their effectiveness in detecting defects and providing strain distribution information since this sensor can monitor throughout its length. This feature differentiates it from other types of sensors. Studies employed OBR sensors to continuously monitor strain along the vessel's axis and detect damage events. OBR sensors were embedded in hybrid structure CPVs, proving capable of detecting impacts and accurately localizing damage. Additionally, OBR sensors were applied in composite tubes for surface mechanical deformation measurement, showing promising results in strain measurement. The performance of OBR sensors was verified through hydraulic cycling testing and acoustic emission sensors in type IV CPVs. Note that, the loading type in CPVs instrumented with distributed fiber optics evolved over the years from hydrostatic tests to impact and cyclic burst tests. Despite the promising potential demonstrated by OBR sensors, challenges persist in optimizing their performance and addressing limitations such as susceptibility to environmental factors and complex signal processing requirements.

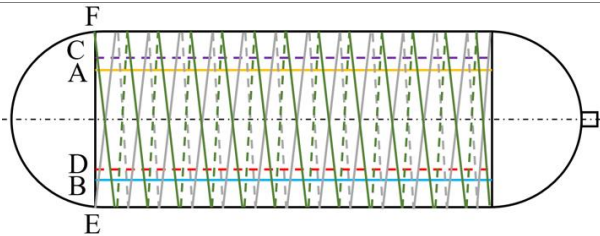

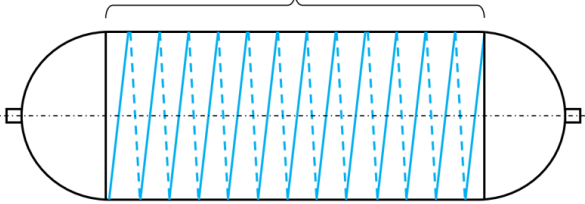
Several studies have explored the integration of FBG sensors into CPV for SHM applications. Researchers installed FBG sensors mainly in composite pipes [60], [76], [143], types III [75], [92], [131], [132] and IV [4], [42], [61], [142], and punctually in type V [70] CPVs. Due to their promising response in measuring deformations, and temperatures and detecting defects, some researchers have tended to instrument a type IV multi-spherical cryogenic tank with FBG sensors. FBG sensors were embedded in the interface between the liner and composite overwrap, highlighting their potential for strain monitoring despite concerns regarding fragility. They were also employed for structural strain monitoring in composite tubes, showing their success in comparison with strain gauges and finite element analysis. In all types of vessels for hydrogen or methane storage, FBG sensors proved sensitive to defects during testing. In addition, FBG sensors were able to monitor continuously the manufacturing and operation phases of the vessels. The use of FBG sensors for measuring strain changes in filament-wound products confirmed their reliability. For torque-induced strain recording in composite cylindrical shaft structures, FBG sensors exhibited sensitivity and applicability in shear-dominated load cases. Employed with a digital image correlation technique for defect detection and deformation measurement in high-pressure vessels, FBG sensors proved suitable for SHM applications. FBG sensors demonstrated effectiveness as quality control tools. Finally, FBG sensors utilized for temperature and strain measurement in composite tanks proved reliable in cryogenic and room temperature environments.

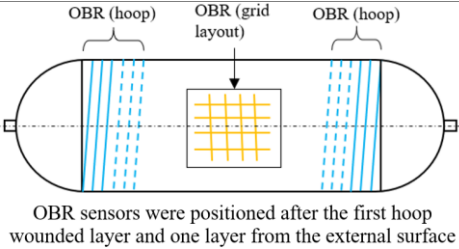
These findings collectively underscore the efficacy of FBG sensors in various CPV applications, providing valuable insights for the development of robust SHM systems.

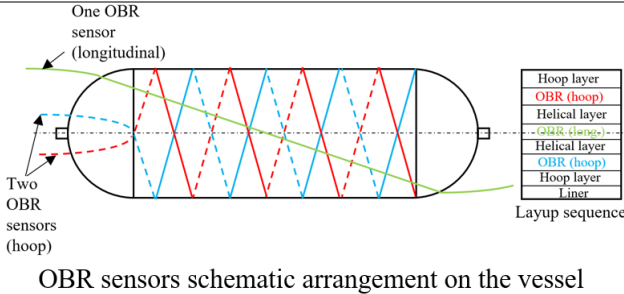
All the recent studies for fiber optics integration in CPVs are detailed and summarized in Table 3, in a chronological way and the ascending degree of use.

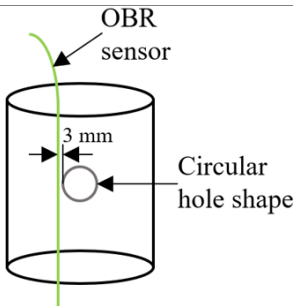
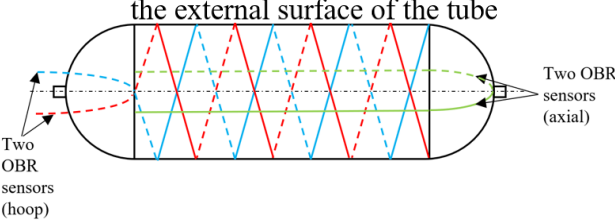
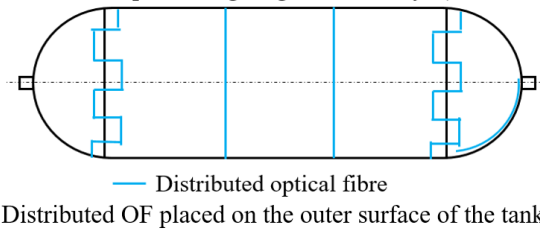
Table 3. Fiber optics sensors integration in CPVs

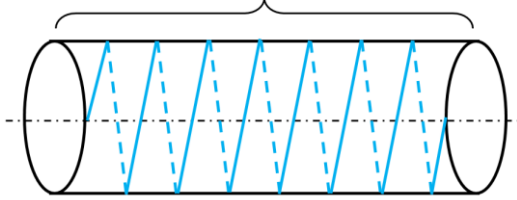
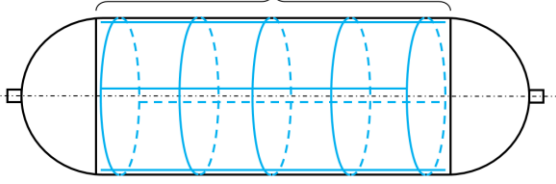
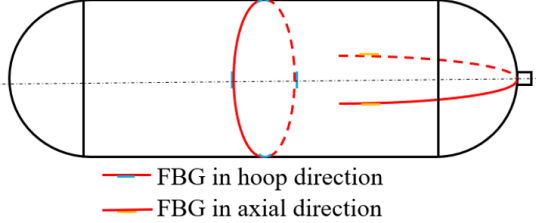
Year	CPV's type and materials	Monitored and controlled parameters	FO sensors layout design and arrangement in CPV	Loading type	Principal conclusions	[Ref]
Interferometric SOFO sensor						
2004	Type IV Liner: polymer Hybrid composite overwrap: carbon fiber-thermoset resin followed by glass fiber layers in the cylindrical section.	Strain measurement for damage detection on the cylindrical section.	<p>SOFO (helicoïdal)</p>  <p>SOFO (axial) with 90° shifting angle between them SOFO sensors embedded between the last carbon fibre layer and the first glass fibre layer</p>	Hydrostatic burst, cyclic, and temperature tests	<p>A linearity between the pressure variation and the average strain measurement was shown.</p> <p>The damage was successfully detected thanks to a developed algorithm.</p>	[73]
2010	Type III Liner: steel Composite overwrap: glass fiber layers-epoxy.	Strain measurement for damage detection on the cylindrical section.	 <p>SOFO®: axial SOFO®: Hoop</p> <p>Two SOFO® sensors (axial and hoop) SOFO sensors were embedded between the last two plies</p>	Hydrostatic burst test	Similar changes in strains were measured by FBG and SOFO®.	[130]

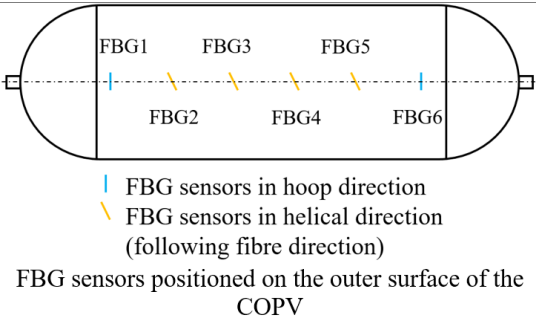
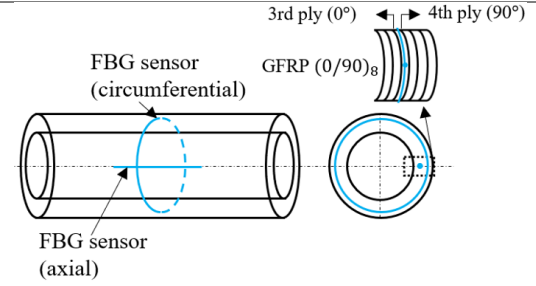
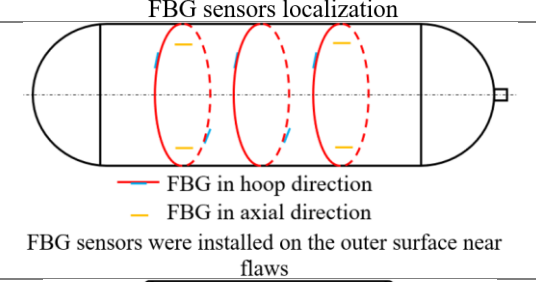
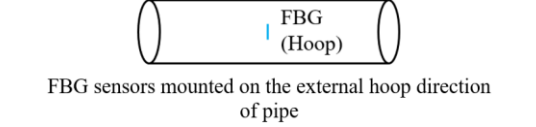
2013	Type III Liner: steel Composite overwrap: carbon fiber.	Strain measurement during the manufacturing and service on the cylindrical section.		Hydrostatic burst and cyclic tests.	SOFO® sensors are less sensitive to defects than FBG sensors.	[129]
Distributed FO sensor						
2014	Type IV.	Strain measurement and defects detection and localization on the whole vessel.		Hydrostatic burst test.	OBR sensors can detect defects at any point of the vessel and provide information about strain distribution.	[133]
Fiber optics arrangement OBR (hoop)				Hydrostatic burst test.	OBR sensors are capable of delivering explicit strain profiles over the cylindrical part of the CPV.	[134]
2016	Type III, Liner: aluminium Composite overwrap: carbon fiber-epoxy followed by glass fiber-epoxy.	Strain measurement, damage detection, and localization on the cylindrical section of the CPV.	OBR sensors located on the carbon-glass fibre composite layers interface		They provide a damage impact localization on the CPV depending on the revealed strain profiles.	

2019	<p>Type III, Liner: steel domes and cylindrical polyethylene mandrel Composite overwrap: carbon fiber- epoxy layers Composite stacking sequence: $[90^{\circ}_2/(\pm 15^{\circ})_2/90^{\circ}_2]$</p>	<p>Strain measurement during an impact test using an impactor on the cylindrical section.</p>	 <p>OBR (hoop) OBR (grid layout) OBR (hoop)</p> <p>OBR sensors were positioned after the first hoop wounded layer and one layer from the external surface</p>	<p>Impact and hydrostatic burst tests.</p>	<p>The hoop placement configuration is the most effective method to detect impacts.</p>	[71]
				<p>The grid method is useful to detect the spreading of impact damage.</p>		
				<p>OBR fiber optic can precisely locate the impact.</p>		

2021	<p>Type IV Liner: polyethylene Composite overwrap: carbon fiber.</p>	<p>Visible impact damage detection, pressure monitoring, and strain profile measurement along the entire vessel.</p>	 <p>One OBR sensor (longitudinal)</p> <p>Two OBR sensors (hoop)</p> <p>Layup sequence</p> <ul style="list-style-type: none"> Hoop layer OBR (hoop) Helical layer OBR (long) Helical layer OBR (hoop) Hoop layer Liner <p>OBR sensors schematic arrangement on the vessel</p>	<p>Impact and hydrostatic burst tests</p>	<p>The embedded OBR sensors are an adequate instrument to detect visible impact damage and monitor an internal pressure.</p>	[136]
				<p>OBR sensors can also monitor the strain profile along the whole vessel.</p>		
				<p>A more effective measurement with less noise can be obtained when the FO is aligned with the reinforcements.</p>		

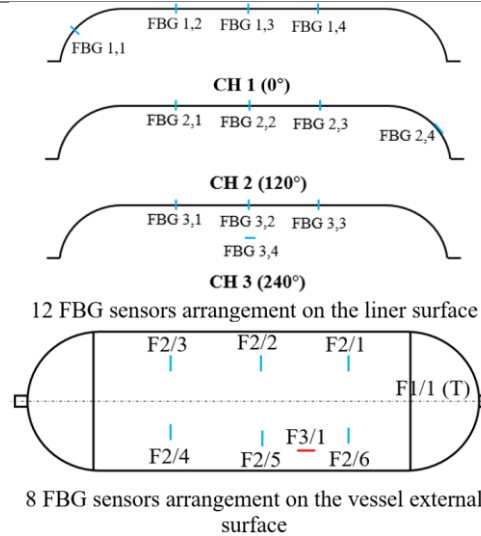
2021	Composite tubes fabricated by carbon fiber-reinforced thermoplastic resin.	Strain measurement on the external surface of the vessel and close to the cut-out circular hole.		Hydraulic biaxial test.	The measured strains using OBR sensors while experimenting were in good accordance with numerical FEA results.	[135]
OBR optical fibre placement behind the circular hole on the external surface of the tube				Hydrostatic burst and cyclic tests.	Validation of OBR distributed sensors with AE technique, as a good tool for strain sensing.	[72]
2022	Type V Composite tank with T700 carbon fiber with a metallic ring on the middle part of the cylindrical section.	Strain and temperature measurements in the transition section.		Cyclic pressurization followed by cryogenic hydrostatic tests.	Not discussed in the experimental results.	[69]

2024	Composite tube: carbon fiber-epoxy layers.	Full-field strain measurement.	Distributed OF Rayleigh scattering technology	Hydraulic static loading.	The embedded OBR sensor effectively captures the strain changes in the middle of the cylinder structure, which aligns with results obtained from the strain gauges and finite element simulation.	[155]	
							
			OF sensor is embedded in a helical way along the fibres (located between the second and third layer of composite)				
2024	Type IV Liner: not mentioned Composite overwrap: carbon fiber reinforced polymer	Strain measurement along the vessel length and circumferential direction on the cylindrical part.	Distributed OF Rayleigh scattering technology	Cyclic hydrogen test.	The strain recorded by the FO sensor measurement has higher values than the strain gauge measurement due to the difference in the quantity of the bonding adhesive between them.	[156]	
							
			Nine distributed OF sensors (bonded on the outer surface): five placed circumferentially and four placed axially with 90° angle between them				
Fiber Bragg Grating (FBG) sensor							
2010	Type III Liner: steel Composite overwrap: glass fiber-polypropylene	Strain measurement.			Cyclic internal pressure loading.	FBG fiber optic presents a good solution to detect strain change, but it needs some concerns for its applicability because it is fragile.	[92]
			<p>— FBG in hoop direction</p> <p>— FBG in axial direction</p>				
			FBG sensors layout on the liner-composite interface				

2010	Type III Liner: steel Composite overwrap: glass fiber layers-epoxy.	Strain measurement and damage detection on the cylindrical section.	 <p>FBG1 FBG3 FBG5</p> <p>FBG2 FBG4 FBG6</p> <p>— FBG sensors in hoop direction — FBG sensors in helical direction (following fibre direction)</p> <p>FBG sensors positioned on the outer surface of the COPV</p>	Hydrostatic burst test.	FBG sensors can monitor strain changes due to any kind of defect detection and can be applied for SHM.	[130]
2011	Composite tube: Glass fiber reinforced polymer with a stacking sequence of $[0/90]_8$	Local strain measurement.	 <p>3rd ply (0°) 4th ply (90°)</p> <p>FBG sensor (circumferential)</p> <p>FBG sensor (axial)</p> <p>GFRP $(0/90)_8$</p>	Inner pressure test and outer concentrated load force.	FBG sensor is a successful tool for in-service SHM of composite tubes.	[141]
2013	CPV Type III, Liner: steel Composite overwrap: carbon fiber epoxy.	Strain monitoring during the manufacturing and in service on the cylindrical section.	 <p>FBG sensors localization</p> <p>— FBG in hoop direction — FBG in axial direction</p> <p>FBG sensors were installed on the outer surface near flaws</p>	Hydrostatic burst and cyclic tests.	FBG sensors are very sensitive to defects.	[129]
2014	Composite tube, Liner: aluminium Composite overwrap: carbon fiber-epoxy.	Local strain measurement.	 <p>FBG (Hoop)</p> <p>FBG sensors mounted on the external hoop direction of pipe</p>	Hydrostatic burst test.	FBG sensor is a reliable and effective tool for measuring the strain.	[59]

2018 Type IV,
Liner: PE
Composite overwrap:
carbon fiber reinforced
plastic.

Liner's deformation,
curing temperature
and time (resin
parameters), vessel
deformation, and
fiber tension
(residual strains).

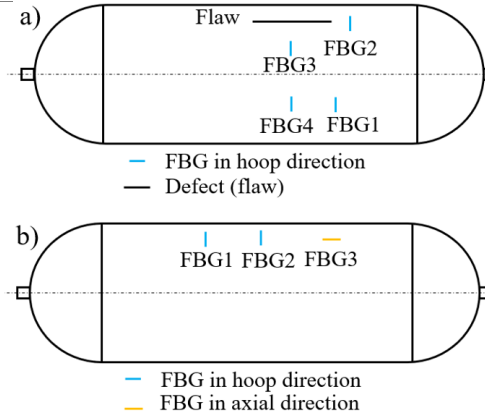


Hydraulic
cyclic test.

Curing process optimization by [4]
setting the appropriate duration
time and the optimal
temperature.

2018 Type IV
Liner: polymer
Hybrid composite
overwrap: carbon and
glass fiber-epoxy.

Strain measurement,
defect localization,
residual strain, fiber
tension, internal
pressure, and resin
polymerization
temperature.



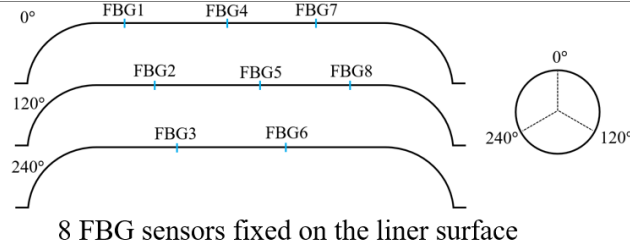
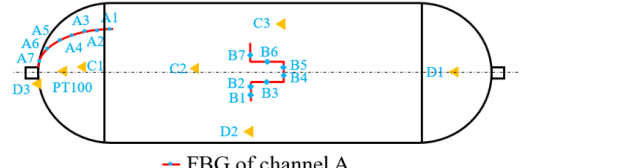
Hydrostatic
burst pressure
test.

FBG sensors afford a [60]
continuous measurement of
strain on multiple points and
detect and localize defects on
the macro CPV scale.

FBG sensors offer registration
of residual strain for composite
structure's quality assessment.

Sensors were attached to the outer surface near flaws

<p>2019 Type IV multi-spherical CPV, Liner: polyamide, Composite overwrap: carbon fiber, Composite sphere layup: [0,45,-45,90]s</p>	<p>Temperature and strain measurements on the outer tank surface.</p>		<p>Hydrostatic burst and cyclic pressure test.</p>	<p>The obtained strain recordings using FBGs were verified with the finite element analysis (FEA) in [70]. [140]</p>		
<p>Layout of FBG sensors on the tank surface Sensors were glued to the external surface</p>		<p>2021 Composite cylindrical shaft fabricated by carbon fibers/epoxy [±55°, ±55°, ±86°, ±55°, ±55°, ±86°, ±55°, ±55°]</p>	<p>Torque-induced strain monitoring.</p>	<p>— Aligned with fibre orientation — Circumferential direction — Axial direction</p> <p>FBG1, 3, 5 were embedded among composite layers and FBG2, 4 were surface-mounted</p>	<p>Static torsion load.</p>	<p>Results showed that maximum sensitivity is recorded for sensors aligned with carbon fibers. [75]</p> <p>Surface-mounted results constitute a viable option for strain monitoring induced by torque.</p>
<p>2021 Type IV Liner: high-density polyethylene, Composite overwrap: carbon fiber composite.</p>	<p>Strain measurement and damage detection and identification.</p>	<p>— FBG in hoop direction — FBG in axial direction</p> <p>FBG sensors fixed on the liner surface</p>	<p>Hydraulic cyclic test.</p>	<p>FBG sensors can be employed in shear-dominated load cases. [41]</p> <p>FBG sensors can be used for the detection of defects and measuring of liner's deformation. Results were confirmed with the FEA model.</p>		

2022	<p>Type III Liner: 6061-T6 aluminium, Composite overwrap: carbon fiber epoxy, Composite stacking: $[90_3/\pm 15_2/90_3]$</p>	<p>Strain measurement during winding for quality control, impact detection, and localization.</p>	 <p>8 FBG sensors fixed on the liner surface</p>	<p>Impact test.</p>	<p>The integration of the FBG sensor array in the liner is a valuable technique for recording the full production process.</p> <p>FBG sensors can be used to take preventive measurements of damage detection and localization.</p>	[74]
2022	<p>Type V Composite: T700 carbon fiber with a metallic ring on the middle part of the cylindrical section.</p>	<p>Strain and temperature measurements.</p>	 <p>— FBG of channel A — FBG of channel B ◀ FBG temperature sensors</p> <p>FBG sensors arrangement on the outer surface of the vessel</p>	<p>Cyclic pressurization followed by cryogenic hydrostatic tests.</p>	<p>FBG sensors based on strain measurement are qualitative sensors to be used in cryogenic or room temperature.</p>	[69]

5- Mechanical impact and composite degradation due to embedded sensors

The degradation of mechanical properties in fiber-reinforced polymer composites is a significant challenge when embedding sensors within the material. This is mainly due to a mismatch in mechanical properties and poor interface properties, where the degradation generally occurs [82], [159], [160]. No matter the integration method used, inserting a sensor into the composite material causes a gap between layers, forming a resin pocket around it. This depends on the shape and size of the object. The effect of sensors integrated into the structure may be harmful and cause premature failure of the CPV structure. In the literature, we can find numerous works exploring the impact of embedding piezoelectric, piezoresistive, and fiber optic sensors in composites. Therefore, in this paper, the impact of embedding these sensors is investigated. The target of this investigation is to overcome or reduce as much as possible the negative effect of embedding sensors on the material's properties degradation.

The composite is a heterogeneous medium. Under mechanical loading, the resin is weak in tension and strong in compression; the fiber is weak in compression and strong in tension. The combination of these two materials ensures the best properties of each component. In consequence, a zone rich in one of these two components is a weak zone. The fact that plies just above and below the inclusion "sensors" are continuous and possess a bending stiffness implies that they cannot perfectly surround the surface of the inclusion [161]. For that, sensors embedded in a composite medium are generally surrounded by a resin-rich region or resin pocket. This local wave caused by resin pocket disturbs not only the values of the field variables measured (stresses, deformations, etc.) but also may cause inter-laminar damage because it acts as a discontinuity in the composite [161], [162], [163], [164]. The form and size of the resin pocket depend on the diameter or shape of the sensor, the stacking sequence, and the filament winding tension force.

5.1- Piezoelectric

PZT sensors have been integrated into a composite material before its manufacture in such a way as to monitor its health in situ. To do this, it is necessary to use sensors as small as possible and in particular with small thicknesses. Regardless of the integration technique, when a foreign body is incorporated into the material, a degradation of its mechanical characteristics can be observed [165]. This degradation is more severe if the wrong integration technique is chosen. The choice of the integration method of the piezoelectric sensor depends mainly on the sensor itself (shape and size) and the existing defect detection field.

For a laminated composite, two techniques for implanting piezoelectric sensors are described in the literature [166], [167]. The first consists of cutting a part of the composite reinforcements at the location of the sensor and integrating it during its manufacture called "cut-out". This method doesn't generate resin-rich pocket regions around the sensor and researchers [168], [169] have demonstrated that PZT incorporation in the heart of laminates glass fiber with epoxy reduces slightly their mechanical strength in static and fatigue. However, it is impossible to use this method during tank manufacturing because the fibers cannot be cut while performing the filament winding process. The second technique is to insert the sensor directly between the layers of the composite without cutting the fibers. In this way, a resin pocket will form around piezoelectric sensors which correspond to the case of FOs embedment in perpendicular direction with respect to the reinforced fibers. Another problem is its flat shape, which may cause a delamination between the two adjacent plies to the sensor.

Hufenbach et al. [94] have studied experimentally by a tensile test the damage caused by piezoelectric sensor embedment in glass fiber-reinforced epoxy specimens. They observed no initial damage in the sensor zone, as shown in Fig. 13 (a), but noted delamination just before final failure, depicted in Fig. 13 (b). They found a degradation of 5 to 10% for the stiffness and 5 to 20% for the tensile strength.

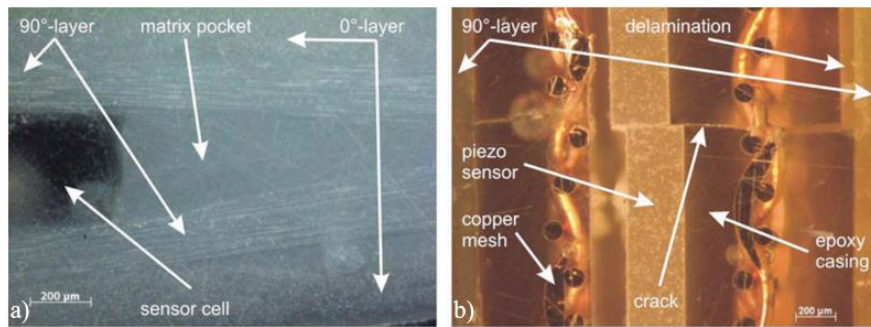


Fig. 13. Microscopic graphs of a [0/90]_s tensile specimen with embedded piezoelectric sensor: (a) after manufacturing; (b) after final failure [94]

Huang et al. [170] have realized a numerical analysis of the stress concentrations that occur at the level of a sensor with a rectangular shape. This sensor is integrated into a unidirectional glass fiber composite. Under tension loading, a stress concentration has been produced at the corner of the sensor due to the geometry and discontinuity of materials near the sensor. This stress concentration may initiate a matrix cracking on the sensor's corner on the interface resin-sensor coating. Konka et al. [171] have examined the impacts of embedding piezoelectric sensors (PZT) on the integrity of composite laminates made of glass fiber with epoxy resin. They conducted a numerical simulation to investigate the stresses across the embedded PZT sensor in the composite. The numerical study demonstrates that high-stress concentration is located on the corner edge of the sensor. The tensile test applied on composite laminates with embedded PZT showed a reduction of ultimate strength by 6%. Finally, they concluded that PZT sensors are not well-compatible with composite laminates. Lammens et al. [172] presented a finite element approach for resin pockets modeling around random and arbitrary inclusions in terms of geometries (square and curved) and materials (silicone and epoxy) embedded in composite materials. These inclusions have somehow the shape of piezoelectric sensors. They compared the force-displacement curve predicted in finite elements with the one measured in experimental tests. They performed 3-point and 4-point bending tests with the inclusion location close to the tension and compression side. The resultant finite element model predicts accurately the resin pocket geometry and presents a prospect for exploring different geometries to get the optimal geometry of inclusion.

Piezoelectric sensors have been integrated into composite materials for in situ health monitoring, requiring minimal sensor size and thickness to mitigate mechanical degradation. The integration technique significantly impacts the composite's mechanical properties. Two primary methods for embedding PZT sensors in laminated composites are described: the "cut-out" method, which involves cutting composite reinforcements to embed the sensor and does not create resin-rich pockets, though it's unsuitable for filament winding processes; and direct insertion between composite layers, which forms resin pockets and may cause delamination. Studies have shown varied effects on mechanical strength, with tensile tests revealing degradation in stiffness and tensile strength. Numerical analyses highlight stress concentrations at sensor corners, leading to potential matrix cracking.

5.2- Piezoresistive

Xiao et al. [173] studied the effect of embedded thin-film cells of 0.1 mm thickness within carbon fiber composite laminates. This film thickness can be considered as a flexible printed circuit. A resin-rich region is formed around the device and its geometry increases when it's embedded near transversal direction plies. The results show that the tensile strength of the composite was reduced by 6%. However, the stiffness demonstrated negligible change and it remain almost unaffected. The decrease in tensile strength is the consequence of a delamination initiation and propagation near the device. Javdanitehran et al. [174] studied the effect of embedded printed circuit board (PCB) sensors on the mechanical behavior of glass fiber-reinforced polymer structures. The PCB plays the role of a flexible printed circuit. The embedment of this sensor generates a resin-rich zone in the surroundings of the sensor. This

resin-rich region causes stress concentration around the sensor and forms a site for the initiation of damage, which may lead to delamination. Several factors influence the geometry and size of the resin-rich zone such as the stacking sequence, number of plies, and thickness of the sensor. Thicker sensors may lead to higher ply waviness which reduces the bending and tensile strength. The ply waviness angle increases with decreasing number of the plies (see Fig. 14 a and b). The contribution of the sensors to the whole tensile modulus of the specimens is negligible in the unidirectional laminate (0°_4). This is due to the higher tensile modulus of the plies. When the tensile modulus of the laminate is smaller than that of the sensor, the sensor impact negatively the stiffness of the laminate and it gets worse with the increased size of the sensor.

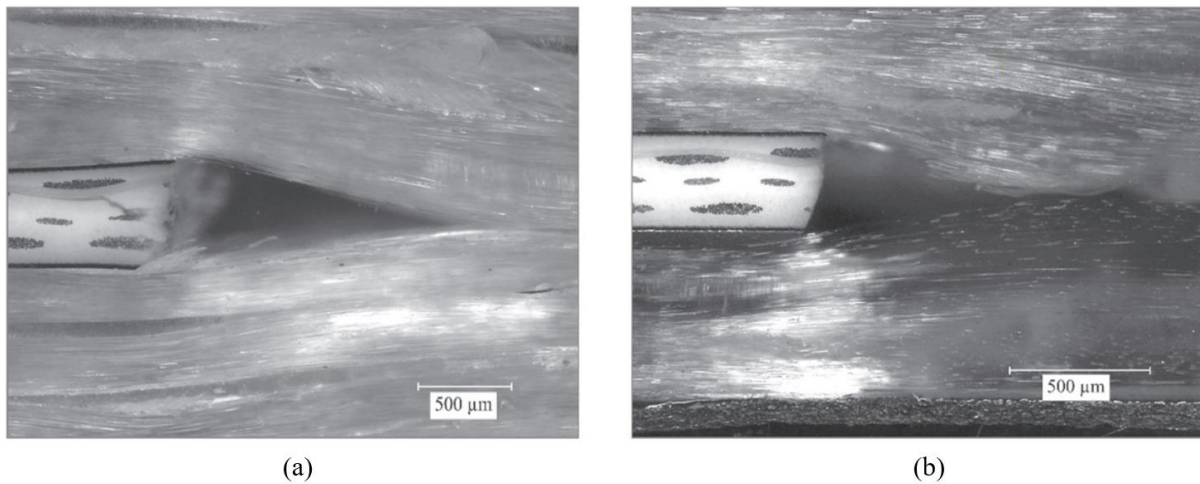


Fig. 14. Resin rich region formation in unidirectional plies: (a) 10 plies; (b) 6 plies [174]

Chen et al. [175] studied the impact of the embedment of piezoresistive sensors in glass fiber-reinforced composite. They embedded mesh film and solid film MWCNT sensors in specimens to test them in tension and bending. The results show that the embedded mesh film has a negligible impact on the mechanical properties of the composite. However, the solid film sensor leads to a severe decrease in both tensile strength (-15.6%) and flexural strength (-35.5%). Thus, the embedment of film cells may also create a resin-rich region depending mainly on the thickness of the film and the orientation of the adjacent layers. The embedding of such sensors affects negatively the mechanical properties of the composite like strength and stiffness.

Embedding thin film piezoresistive sensors within carbon fiber composite laminates forms resin-rich regions that can reduce tensile strength due to delamination, although stiffness remains unaffected. The presence of PCB sensors in glass fiber-reinforced polymers creates stress concentrations around the sensors, leading to potential delamination, with the impact influenced by factors such as stacking sequence, ply number, and sensor thickness. Thicker sensors intensify ply waviness, reducing bending and tensile strength. Piezoresistive sensors embedded in glass fiber composites show that mesh film sensors have minimal impact, while solid film sensors significantly decrease tensile and flexural strength, highlighting the importance of sensor flexibility and thickness, and layer orientation in preserving composite mechanical properties.

5.3- Fiber optics

Integrating sensors among composite layers is crucial for data quality and structural integrity, affecting material properties. Theoretically, the stiffness and strength degradation of composites depend mainly on the angle between FO and reinforced adjacent plies, and FO diameter [130].

Previous studies were carried out to characterize the effect of FO sensor embedment in the bulk of the composite structure. In this paper, the extreme two cases are presented, firstly when the FO is parallel to the reinforced fiber (FO is in the same direction as reinforced composite fiber) and secondly when

the FO is perpendicular to the reinforced fiber. The mechanical properties of the host composite evolve with respect to the angle between FO and the adjacent plies. When the angle between FO and adjacent plies decreases, the mechanical properties of the composite are enhanced.

In the first case, the angle between the FO and the reinforced fibers is 0° . It is noted in the literature that the distribution of reinforced fiber around the FO is uniform [176]. Therefore, this type of FO orientation can minimize the defects and alteration of the mechanical properties. In this context, the FO plays the role of a reinforced fiber and hence it supports a part of the loading. From this point of view, this integration method has little impact on the resistance and modulus of the structure even if FO sensors are positioned in critical zones [72], [177], [178].

However, the severity of the material's properties impairment increases as the angle between the FO and the nearest ply direction rises, to attain a maximum value of 90° which corresponds to the worst case of placing the FO perpendicularly or transversally to the reinforced fiber direction [179]. This results in the formation of an "eye" configuration and voids in the resin, representing a resin pockets geometry on the FO surroundings [162], [164], [180], [181], [182]. The modulus of elasticity of the resin pocket is significantly lower than the host composite. In consequence, the resin pocket acts as a "hole" in the structure and can lead to ruin by delamination [130]. Fig. 15 a and b show a micrograph image of the cross-section of unidirectional composite laminate with FO embedment.

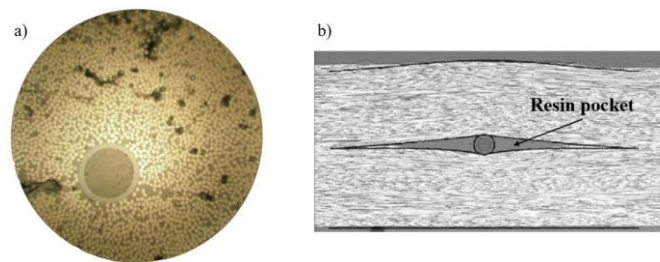


Fig. 15. Micrograph images of FOs embedded in unidirectional (UD) composites : (a) FO parallel to CFRP [39]; (b) FO oriented perpendicularly to UD composite direction [164]

Another factor that can intensify the degradation of the mechanical performance of composite material is the diameter of the FO. Ramakrishnan et al. [130] have reported that because the outer diameter of FO is 10 to 15 times larger than reinforced fibers, it acts as a localized defect which may cause the failure of the composite structure. To overcome this problem, FOs with a small outer diameter of $90 \mu\text{m}$ may be used. The size of the resin pocket is directly proportional to the FO diameter and the bending stiffness of the host composite material. In other words, resin pocket length tends to increase with the diameter of FO and the bending stiffness of composites. Sharma et al. [3] have introduced the filament winding machine parameters that play a significant role in the performance of the vessel in terms of better weight performance, minimum winding defects, and high fiber volume fraction. They mentioned that the tension applied on the fiber while performing the filament winding process has an important effect on the structural performance of the tank since it affects the fiber volume fraction of the composite material. Rising the fiber tension induces a deformation, which can squeeze the polymer resin out increasing the fiber volume fraction. In other terms, lowering the tension of fiber is incapable of removing the excess quantity of resin which yields resin pocket formation around FO sensors.

Ma et al. [183] published an article concerning the prediction of resin pocket geometry created around the inclusion of rigid fiber in a composite laminate. They analyzed the influence of stacking sequence and the angle of plies close to the inclusion on the size of the resin pocket. They conducted an experimental study by comparing the size of resin pockets for six different stacking sequences. The rigid fiber (inclusion) was embedded at the level of a symmetrical plan for each sequence consisting of eight plies. The angles of plies near the inclusion are 0° , 15° , 30° , 45° , 60° , and 75° ; where 0° corresponds to the configuration where the orientation of plies near the inclusion is perpendicular to the direction of the

rigid fiber inclusion. The relative length of the resin pocket is characterized by ($a^* = a/r_0$), where a is the width of the resin pocket and r_0 is the radius of the inclusion as shown in Fig. 16 a. They found that the angle of plies near the inclusion has a greater influence compared to those far from inclusion. Hence, the size of the resin pocket depends largely on the plies close to the inclusion. Consequently, the size of the resin pocket decreases when decreasing the angle between the inclusion and adjacent plies orientation until they are aligned and have the same orientation to get the minimum size of the resin pocket, as can be seen in Fig. 16 b. Thus, to minimize the degradation of the composite's structure performance, the size of the resin pocket must be minimized as much as possible. To ensure this condition, the smallest possible diameter of FO must be used and the FO sensor should be embedded near the plies having the smallest possible angle between them.

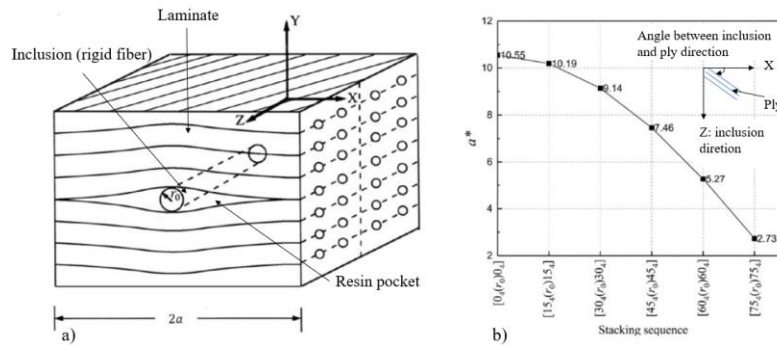


Fig. 16. Inclusion embedment in a laminate: (a) resin pocket schematization; (b) variation of the relative length of resin pocket with the angle between inclusion and plies orientation [183]

Al-Shawk et al. [162] evaluated stress concentrations in the resin pocket considering different diameters and forms of vascular channels. These channels play the role of FO sensors. On the one hand, they have studied numerically the effect of variation of four diameters (0.4 mm, 0.6 mm, 0.8 mm, and 1 mm) embedded in the following four stacking sequences: $[0]_{16}$, $[90]_{16}$, $[90/0]_{45}$ and $[0/90]_{45}$. They showed that a larger vascular diameter induced higher stress regions. They also studied the effect of two shapes of vascular channels “circular and elliptical” on the stress concentration at the resin pocket. A decrease in stress is observed near the vascular when an elliptical configuration is used instead of a circular one despite having the same cross-section. This reveals the advantage of using elliptical instead of circular vascular shapes for lower stress concentrations. Fig. 17 a shows the model geometry, boundary conditions, and loading. Fig. 17 b, c, d, and e illustrate the longitudinal stress distribution in the resin-rich pocket for a vascular diameter of 1 mm, corresponding to $[0/90]_{45}$, $[90/0]_{45}$, $[0]_{16}$ and $[90]_{16}$ stacking sequences, respectively. It was revealed that for UD 90° the stresses are more concentrated near the vascular area; which is not the case for UD 0° where a homogeneous distribution takes place. Concerning the $[90/0]_{45}$ and $[0/90]_{45}$ stacking sequence, stresses have values between these two extremes. Fig. 17 f, g, h, and i represent the stress contour in the resin-rich region in the case of $[0/90]_{45}$ stacking sequence for various vascular diameters of 1 mm, 0.8 mm, 0.6 mm, and 0.4 mm, respectively. As can be seen, the zone of higher stress is larger when the vascular diameter is 1 mm compared to other smaller diameters. At the top of the vascular channel (point B as mentioned in Fig. 17 a), the longitudinal stress is higher compared to the one close to point C. Fig. 17 j and k represent the longitudinal stress contours for 1 mm circular vascular size and a vascular elliptical shape, respectively. A drop of stress was observed close to the elliptical form of the vascular channel compared with the circular one at the level of the resin-rich pocket.

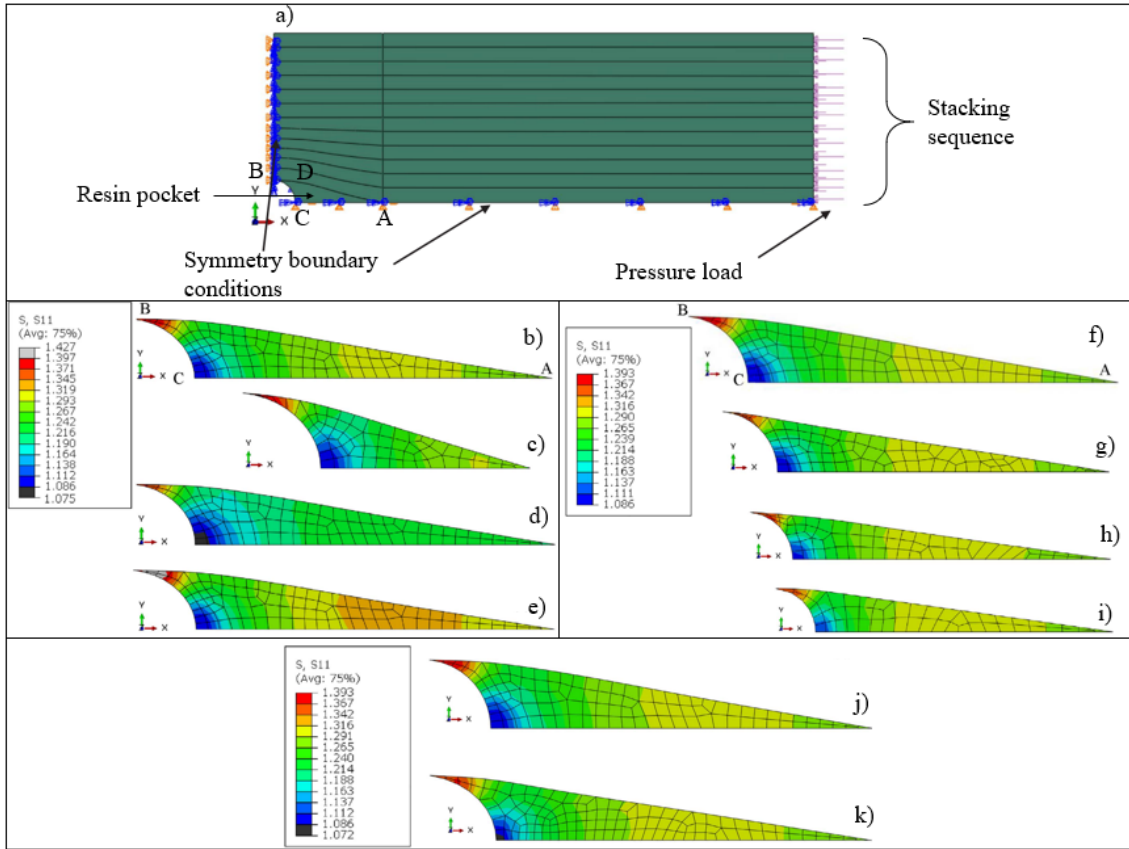


Fig. 17. Longitudinal stress contours at the level of resin pocket region near a vascular channel embedded in a different composite stacking sequence: (a) geometrical model with boundary conditions and loading; for a vascular diameter of 1 mm (b) $[0/90]_{4S}$; (c) $[90/0]_{4S}$; (d) $[0]_{16}$; (e) $[90]_{16}$; for a stacking sequence of $[0/90]_{4S}$ the vascular diameter (f) 1 mm; (g) 0.8 mm; (h) 0.6 mm; (i) 0.4 mm; (j) 1 mm circular vascular size and (k) a vascular elliptical shape with the same cross-sectional area [162]

Fedorov et al. [182] analyzed numerically the stresses in the vicinity of FBG embedding in 20 layers of carbon fiber-reinforced composite. They conducted a comparative study of FO embedded in a laminated composite with different layer orientations near the fiber optic and a homogeneous orthotropic medium. The following three configurations of stacking sequences were analyzed $[0/0]$ where FO is parallel to reinforced fiber, $[90/90]$ FO is perpendicular to reinforced fiber, and $[0/90]$ as shown in Fig. 18 a. A resin pocket is not formed for the case of parallel embedment of FO to carbon fibers. However, a maximum eye shape of the resin pocket is formed for the case of perpendicular embedment. A load P_0 was applied perpendicular to the FO and parallel to composite layers, and the coordinate axis can be seen in Fig. 18 b. They concluded that the following two conditions can eliminate the formation of resin pocket and stress concentration across the FO: 1) the FO diameter must be less than the thickness of the composite layer; 2) the direction of FO must coincide with the unidirectional layer orientation. They also concluded that the obtained calculation based on the homogeneous model has predicted a high-stress concentration across the FO as shown in Fig. 18 c. Thus, they found that the multilayer model must be used to obtain accurate results of stress concentration.

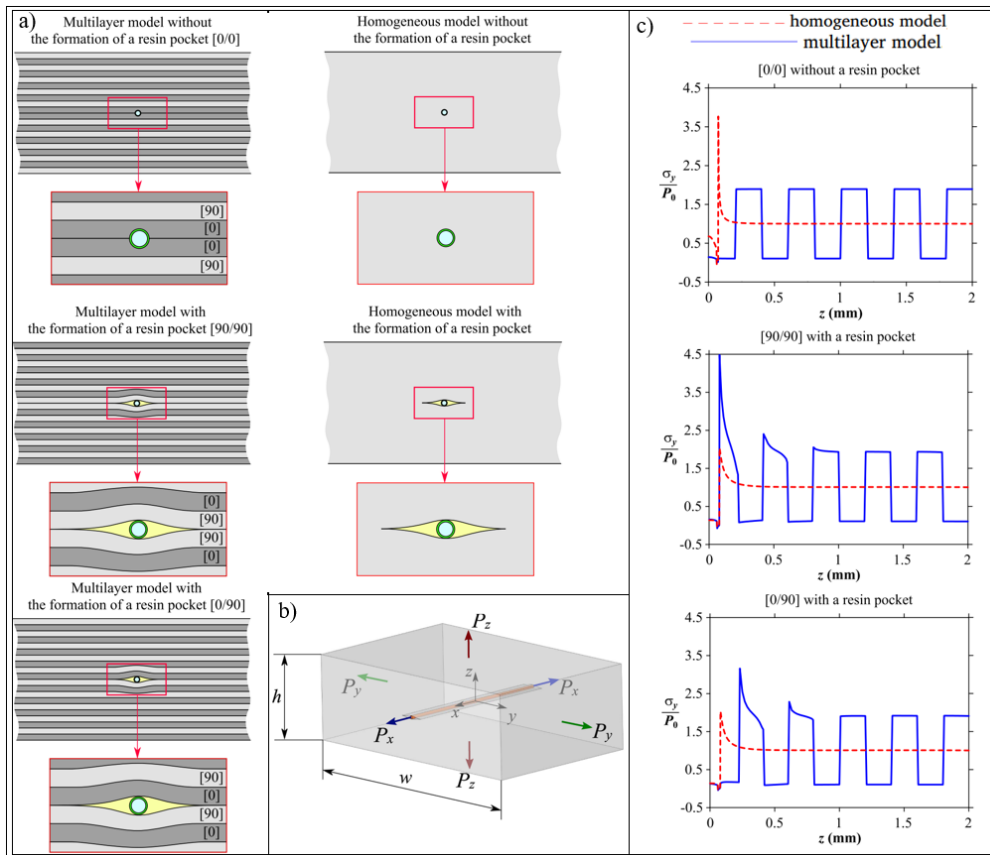


Fig. 18. FO embedded in polymer composite material: (a) representation of each case study regarding the embedment of FO in composite reinforced polymer; (b) coordinate axis; (c) stress distribution across FO [182]

The mechanical properties of composites, such as stiffness and strength, depend on the angle between the fiber optics and the adjacent reinforced plies, as well as the FO diameter. When FOs are aligned parallel to the reinforced fibers, the integration method minimally affects the composite's mechanical properties, as the FOs support part of the load. However, when FOs are embedded perpendicularly, it results in resin pockets and defects, leading to decreased elasticity and potential delamination. Reducing the angle between the FO and adjacent plies, and using smaller diameter FOs, minimizes resin pocket size and preserves the composite's structural performance. Additionally, the tension applied during the filament winding process and the stacking sequence of the plies influence the formation of resin pockets and the mechanical integrity of the composite.

5.4- Mechanical aspects of sensor integration

The mechanical integration of piezoelectric, piezoresistive, and fiber optic sensors into CPVs requires meticulous attention to sensor size, embedding methods, and precise placement to minimize defects and maintain structural integrity. Piezoelectric sensors, known for their high sensitivity in dynamics loading, must be carefully positioned to avoid creating stress concentrations that could impact the integrity of the composite structure; these sensors are typically embedded during the lay-up process, where layers of composite materials are arranged and consolidated. Piezoresistive sensors, which are often smaller and more flexible, necessitate integration techniques that ensure robust adhesion while preserving the mechanical properties of the composite. This is critical to prevent any alterations that could weaken the mechanical strength of the vessel. Fiber optic sensors, valued for their exceptional accuracy and minimal size, are usually embedded along the reinforced fiber paths within the composite matrix. This strategic placement ensures that the sensors align with the structural fibers, providing precise monitoring data without adding significant bulk or creating stress points within the composite. The parallel embedment

of FO sensors along with the reinforced fibers prevents the generation of resin pockets around the sensor which acts as a weak region.

6- CPV's SHM system discussion

6.1- Summary of sensors

This review article provides an overview of the most trending used sensors in the application of health monitoring of composite vessels. Table 4 summarizes and compares the main characteristics of these three types of sensors described above. They are arranged according to their descending degree of use in CPVs application.

Table 4. Main characteristics of sensors used for CPV's monitoring

Sensor's type	Sensor's technology	Specifications and characteristics	Monitored parameters	Mechanical impacts	Advantages	Disadvantages	[Ref]
FO sensors	FBG sensor	<ul style="list-style-type: none"> - Strain resolution $\approx 1 \mu\epsilon$ - Temperature sensitivity $\approx 10 \text{ pm}/^\circ\text{C}$ - Adaptable for cryogenic temperature $\sim -269^\circ\text{C}$ 	<ul style="list-style-type: none"> - Measurements of strain and temperature - Monitoring of the curing process - Detection and localization of damage 	<ul style="list-style-type: none"> - Good compatibility of FO with the host composite - No stress concentration due to the circular shape of the sensors - Elimination of resin pocket with parallel FO 	<ul style="list-style-type: none"> - Discrete and multiple measurements of temperature and strain over enormous areas and at specifically required zone - Largely accepted technology 	<ul style="list-style-type: none"> - Limited assessment of damage location - Cross sensitivity of strain-temperature 	[32], [42], [61], [70], [130], [181]
	OBR technology	<ul style="list-style-type: none"> - Strain resolution $\approx 2 \mu\epsilon$ - Operating temperature $\sim -40 \text{ à } 300^\circ\text{C}$ 	<ul style="list-style-type: none"> - Delamination - Damage - Strain - Temperature - Vibration 	<ul style="list-style-type: none"> - No influence on the stiffness and strength of the material when the FO is placed parallel to the reinforced fibers - Decreases the stiffness and strength by 5% when the FO is placed perpendicularly to the reinforced fibers 	<ul style="list-style-type: none"> - Continuous measurement of profiles at any location along the length of the fiber 	<ul style="list-style-type: none"> - Costly interrogation system 	[32], [72], [73], [130], [181], [184]
	Interferometric (SOFO®) or Fabry-Perot (F-P) sensor	<ul style="list-style-type: none"> - High strain resolution $\approx 0.15 \mu\epsilon$ - Operating temperature -40 to $+250^\circ\text{C}$ 	<ul style="list-style-type: none"> - Monitoring of the curing process - Strain - Temperature - Damage - Vibration 		<ul style="list-style-type: none"> - High sensitivity of temperature and strain - Flexibility of sensor size 	<ul style="list-style-type: none"> - Difficult to multiplexed - Brittle - Cross sensitivity of strain-temperature 	[32], [74], [130], [131], [132], [181]
Piezoresistive sensors	BP and MXene sensors	<ul style="list-style-type: none"> - Strain resolution $\approx 2.68 \mu\epsilon$ - Temperature sensitivity $\approx 0.105/^\circ\text{C}$ 	<ul style="list-style-type: none"> - Damage detection - Thermal and mechanical strain - Change in electrical resistance 	<ul style="list-style-type: none"> - Flexible film sensors have minimal impact, while solid film sensors significantly decrease tensile and flexural strength 	<ul style="list-style-type: none"> - Resistance to shock - Possess good stability - Lightweight - Used in places with high curvature 	<ul style="list-style-type: none"> - Primarily restricted to insulated composite materials 	[32], [65], [67], [113], [114], [115], [173], [185]

				<ul style="list-style-type: none"> - Resin pocket generation due to the shape of the sensor - Stress concentration around the corner of the sensors - Nanocarbon materials bring a mechanical reinforcement effect 	<ul style="list-style-type: none"> - The higher sensitivity of damage for MXene compared to BP 		
Piezoelectric sensors	PZT and PVDF	<ul style="list-style-type: none"> - Strain sensitivity $\approx 5V/\mu\epsilon$ - Operating temperature ≈ -20 to $+60^\circ\text{C}$ 	<ul style="list-style-type: none"> - Strain measurement - Cracks detection - Sensitive to microdamage - Acoustic emission - Damage localization 	<ul style="list-style-type: none"> - Stress concentration around the corner of the sensors - Resin pocket generation due to the shape of the sensor - Decreases the stiffness by 5 to 10 % 	<ul style="list-style-type: none"> - Very cheap - High mechanical strength - High electromechanical response - Small size - Operating in a wide frequency range 	<ul style="list-style-type: none"> - Complex form compared to FO sensors - Long cable connection - Sensitive to high temperatures - Limited to dynamic use 	[32], [62], [63], [92], [94], [156], [186]

6.2- Discussion and prospect

The goal of the proposed discussion is to furnish a SHM system for building a foundation for the upcoming experimental work of researchers. A good SHM system enables precise detection of critical parameters such as strain and temperature, reduces the probability of composite material degradation, and provides appropriate protection of sensors from external environmental effects. The type, number, position, and size of sensors represent significant factors to be identified to define the best SHM system for CPVs. From a mechanical performance point of view; when designing an SHM scheme for CPV, it is crucial to have sensors possess the following features lightweight, small dimensions, adaptable geometry with the host material, little deficiencies induction, high sensitivity, good damage monitoring ability and signal transmission, and preferably low price. This section gives a quick overview of a few concerns to keep in mind while conceiving a SHM system for CPV application.

Piezoelectric sensors such as PZT and PVDF are less commonly used for monitoring CPVs. Piezoelectric sensors are characterized by their high mechanical strength and cost-effectiveness compared to fiber optic sensors. They can be mounted on the vessel's outer surface or embedded within composite layers, enhancing their durability and sensitivity to structural deterioration. Despite their high electromechanical response and versatility in dynamic conditions, piezoelectric sensors face challenges such as reduced effectiveness in static conditions and sensitivity to high temperatures. Their complex form can cause stress concentrations around the sensor corners, and the extensive cabling requirements may negatively impact the structural performance.

Over the past five years, the integration of piezoresistive sensors based on carbon nanotubes thin film networks, such as BP and MXene, has advanced significantly in the field of filament-wound CPVs. Embedding nanomaterial-based sensors for SHM in-situ serves to obtain damage information due to the disruption of the conductive network film, signaling strain in the composite. Nanocarbon material can also provide a reinforcing effect by enhancing the mechanical properties of the composite vessels. This type of sensor can be employed as a self-sensing strategy since it is based on nanocarbon materials. The BP sensor is characterized by its high flexibility, reliability, resistance to shock, and higher sensitivity than the MXene sensor to the onset and propagation of microcracks in the composite part of the vessel. While the MXene sensor could perform multi-directional strain monitoring more accurately than the BP sensor, extremely sensitive to the low energy impact and the compressive residual strains or plastic deformation of the aluminium liner. Despite their advantages, the integration of such types of sensors may create stress concentration around the corner of the sensor which may initiate matrix cracks, create a resin pocket near the sensor due to its shape, and decrease the tensile strength of the composite materials.

Embedding sensors in composite structures can affect their mechanical properties. To address these challenges, several methodologies can be explored to mitigate their mechanical effects:

- Flexible embedding techniques [175], [187], [188], [189], [190]: utilizing flexible embedding methods can help in distributing the mechanical stress more evenly and reduce the impact on the structural integrity of the composite material. Techniques like soft polymer encapsulation and flexible circuit designs can be effective in this regard.
- Adaptive interfaces [191]: developing adaptive interfaces that can conform to the shape and movement of the composite material can minimize stress concentrations around the embedded sensors. This can be achieved through the use of materials with similar mechanical properties to the composite or through design optimizations that allow for better load transfer.
- Low-Profile sensor designs [192], [193]: designing low-profile or thin-film sensors can significantly reduce the mechanical disturbances caused by sensor embedding. These sensors can be integrated with minimal disruption to the composite's structural performance.
- Integrated strain relief mechanisms [194]: incorporating strain relief mechanisms can help in managing the stress and strain around the embedded sensors. These mechanisms can include

the use of buffer layers, compliant materials, or special geometrical features that absorb and dissipate the stresses.

By implementing these methodologies, the adverse mechanical effects of sensor embedding in composite materials can be mitigated, ensuring that the structural integrity and performance of the composites are maintained while achieving effective SHM.

The selection of the sensor's type is of great importance to have the appropriate SHM system. Among the used sensors in the CPV application, fiber optics reveal the top trending sensor to meet the structural integrity requirement of CPV. The choice is made on FOs (FBG ones) sensors thanks to their special geometrical and working characteristics. The FO sensor itself is a fiber that can mix with the other reinforced fibers of the composite shell. Unlike other sensor types, FO sensors have a cross-sectional circular shape which can eliminate the stress concentration across the FO which may cause a matrix crack initiation. Additionally, FBG sensors can perform multiple measurements (ex: strain and temperature) through a single FO due to their multiplexing feature. They have a high sensitivity to monitor damage or strain changes in the structure compared to other sensors.

To complete the design of the SHM system, the number and positioning of FO sensors must be determined in an optimized way. With the help of FEA numerical simulation, the CPV should be simulated in FE software concerning its working conditions (fatigue cycling, bursting, etc.). Based on the analysis of the result's simulation, the number and localization of FO sensors can be then determined in the critical stress concentration zones. Although the embedment of FO sensors among carbon fiber composite layers has notable benefits to detecting efficiently the controlled parameters in real-time, they might create locale discontinuities within the load-bearing composite structure and degrade their mechanical properties. To overcome this problem, the analysis of the recent literature stipulates that wounding more extra glass fiber layers onto the cured carbon fiber reinforced plastic composite layers can solve this problem. This solution takes place when installing FO sensors among the external glass fiber layers which will prevent the negative influence on the strength and fatigue resistance of the vessel as carbon fiber is the main load-bearing. These glass fiber layers serve also as a protective coating layer for sensors against external harsh environmental conditions (temperature, impact, humidity, etc.). One more important thing that affects the strength and stiffness of the composite shell in the vessel is the angle between the fiber optic and the relatively closest composite layers' orientations. Theoretically, placing the FO in parallel with the reinforced nearest plies helps in load carrying, reduces the formation of resin pockets, and maintains a uniform consolidation around the FO, which results in minimizing defects and decreases the deterioration of the composite's mechanical properties. Choosing a smaller diameter of FO can also reduce the formation of resin pockets around the sensor.

Recently, the integration of emerging technologies, such as artificial intelligence (AI), machine learning (ML), digital twins, and advanced data analytics, represent a significant advancement in the field of CPVs [49], [195], [196], [197]. The conducted analysis of publication trends using the keywords "Composite Pressure Vessel" and "Machine learning" between the years 2005 and 2022 underlines this growing interest, highlighting the advancement of this research field. The analysis is limited to some filters including an article document type and an English-language article. As can be seen in the publication trends (see Fig. 19), the degree of use of machine learning-based SHM has been growing largely from the beginning of the year 2020. These technologies are transforming the landscape of SHM by enabling more sophisticated and efficient approaches to predictive maintenance and real-time monitoring. AI and ML technologies need vast amounts of data generated by sensors to develop models and algorithms that can predict the structural health of CPVs with high precision. The algorithms can process and analyze large datasets from SHM systems, identifying patterns and anomalies that may indicate early signs of damage. By learning from historical data, ML and AI models can predict the burst pressure and failure to proceed with the maintenance for service life extension. Therefore, AI systems can automate the diagnostic process, providing real-time insights and recommendations without the need for extensive human intervention [195].

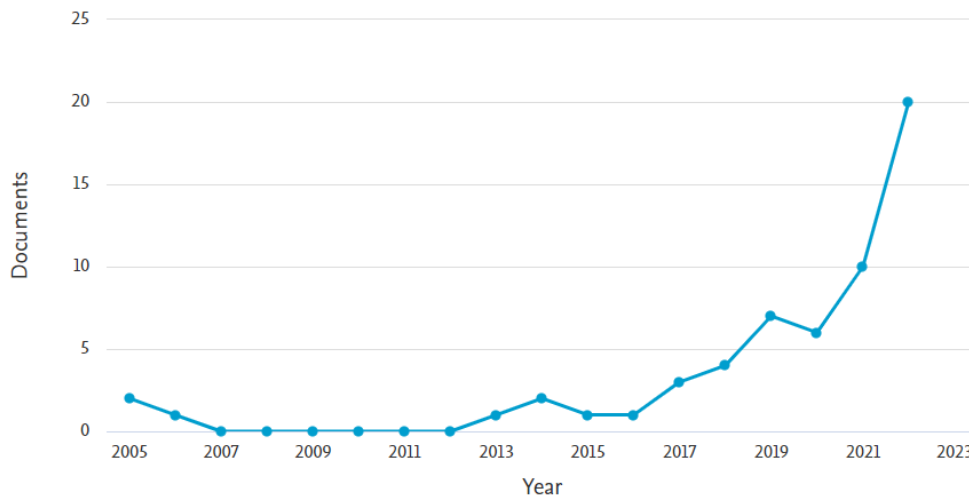


Fig. 19. Documents (publications) in the field of machine learning for composite vessel monitoring

While AI and ML offer promising advancements in the development of CPVs, they also present several challenges. One major issue is the extensive data requirements for AI, where the quality and accuracy of the data significantly impact the model's reliability and effectiveness. In the context of CPV storage, obtaining comprehensive data on their behavior and performance may be limited, presenting a substantial challenge. Additionally, AI models are susceptible to biases, either from the data used or the algorithms themselves, potentially leading to inaccurate predictions or recommendations, which is particularly concerning for safety-critical systems [195].

The analysis of the literature shows that the critical zones of the vessels are mainly in the middle of the vessel, the junction cylinder-dome, near the boss, and the interface liner-composites. This review highlights the significant potential of sensor technologies used for monitoring CPVs. To maximize the practical impact of our findings, it is crucial to translate these strategies into real-world applications. For instance, implementing these advanced sensors in aerospace, automotive, energy, naval, and chemical industries for liquid and gas storage can lead to more reliable and safer CPVs. Future research should focus on optimizing sensor integration methods within CPVs in particular to further minimize their impact on structural integrity and improve their durability in various operational conditions. In addition, SHM has become a growing trend in various industrial sectors. Nowadays, it is widely applied due to its rapid data and signal processing capabilities, providing accurate and reliable information to feed AI and ML models for predictive maintenance.

One of the most significant advantages of implementing health monitoring systems in CPVs is the ability to continuously monitor the state of the structure throughout its entire life cycle. However, CPVs have often been in service for decades and are exposed to various environmental factors such as moisture, heat, and aging. The factors might affect both the sensors and the collected data, raising critical questions about the long-term reliability [198] and accuracy of health monitoring data. The durability of FO sensor is affected by factors like construction work or operator mistakes that can cause cable breaks [199]. In this study [199], a FO sensor was subjected to water and ice for 16 years. As a result, cracks and damage occurred on the polymer coating of the FO sensor. Beyond construction activities, aging might be intensified by other factors: the impact of water [200], [201], and the effect of high-power laser emissions [202], potentially causing permanent harm to the connectors.

The durability of piezoelectric sensors and the reliability of their generated data might be affected also by the aging and degradation of the bonding itself [203], [204]. It was reported a 9% reduction in the static capacitance of PZT after 500 cycles thermal cyclic aging between -55 °C and 85 °C [203]. Humidity and water could induce the degradation of thin-film PZT sensors. PZT sensors are susceptible to humidity, which can accelerate time-dependent dielectric breakdown more than in dry environments

and significantly affect the dynamic performance of PZT devices. For 95% relative humidity, a severe deterioration of the device's dynamic behaviour is depicted [205]. Del Bosque et al. [206] have evaluated the mechanical and sensing performance of piezoresistive sensors under hydrothermal aging. They found that the diffusion coefficient is higher in the case of GnPs adopted samples than MWCNT ones because GnPs present very good barrier properties due to their 2D geometry. Piezoelectric MXene sensors tend to oxidize easily when exposed to water, air, and light, which affects the stability of the sensor [207]. When exposed to those environmental conditions, the metallic electrical conductivity and other properties deteriorate with respect to their oxidation degree.

7- Conclusion

The distinctive aspect of this review lies in its detailed overview of existing studies on the integration of sensors into composite vessels, focusing on different sensor types, their positioning, and their impact on the structural integrity of the vessels. This paper offers a comprehensive review of the most relevant sensors, either available in the market or created in the laboratory for SHM purposes of self-sensing CPVs structures. The goal of this article is to provide information about the types of sensors used for CPVs monitoring. Additionally, it aims to furnish information regarding their integrations into CPVs, including controlled parameters, arrangement, and positioning. Furthermore, the paper addresses the aspect of composite materials degradation due to sensor embedding, emphasizing the importance of SHM strategies that minimize negative impacts on the mechanical performance of composite vessels.

Various sensor technologies including fiber optics (FBG, OBR, and SOFO), piezoelectric (PZT, SMART layers and PVDF), and piezoresistive (BP and MXene) have been explored for monitoring CPVs. FBG sensors are predominantly used in type III, IV, and V CPVs. OBR sensors are used for damage monitoring and strain measurement along the length of the fiber optic in type III and IV vessels, while SOFO sensors have limited applications in CPVs monitoring. Piezoelectric sensors like PZT or PVDF are less common due to their thickness relative to composite layers. Recently, piezoresistive sensors (BP and MXene) have been incorporated in only type III vessels. Sensors integration can be surface-mounted or embedded, with trade-offs between ease of installation and maintenance versus precision and mechanical alteration of the vessel's mechanical properties. Understanding the interaction between sensors and the host composite material is essential for determining an appropriate placement for the embedded sensors.

FBG sensors are the most recommended for CPV monitoring due to their multiplexing capability and minimal impact on mechanical performance. Embedding them among additional layers and parallel to fiber directions enhances the durability and accuracy of the measured parameters. Integrating SHM systems into CPVs enhances safety and reliability, and reduces maintenance costs by enabling continuous, in-situ monitoring throughout the vessel's service life, as these structures operate under critical loadings and temperatures.

Acknowledgments

Publication carried out as part of the CORENSTOCK [208] Industrial Chair ANR-20-CHIN-0004-01, co-founded by the industrial company elm.leblanc "Group BOSCH", IMT (Institut Mines-Télécom), and its Schools IMT Nord Europe and École des Mines de Saint-Étienne, funded by the French National Research Agency, supported by the Carnot Institute Télécom & Digital Society, and endorsed by the EMC2 pole.

References

- [1] P. Sharma *et al.*, « Effects of dome shape on burst and weight performance of a type-3 composite pressure vessel for storage of compressed hydrogen », *Compos. Struct.*, vol. 293, p. 115732, août 2022, doi: 10.1016/j.compstruct.2022.115732.
- [2] S. Alam, G. R. Yandek, R. C. Lee, et J. M. Mabry, « Design and development of a filament wound Composite pressure vessel », *Compos. Part C Open Access*, vol. 2, p. 100045, oct. 2020, doi: 10.1016/j.jcomc.2020.100045.
- [3] P. Sharma, P. Chugh, et S. Neogi, « Study to methodize the design of a safe Type-4 CNG storage vessel using finite element analysis with experimental validation », *Int. J. Press. Vessels Pip.*, vol. 192, p. 104425, août 2021, doi: 10.1016/j.ijpvp.2021.104425.
- [4] P. Gąsior, R. Rybczyński, J. Kaleta, S. Villalonga, F. Nony, et C. Magnier, « High Pressure Composite Vessel With Integrated Optical Fiber Sensors: Monitoring of Manufacturing Process and Operation », in *Volume 5: High-Pressure Technology; ASME Nondestructive Evaluation, Diagnosis and Prognosis Division (NDPD); Rudy Scavuzzo Student Paper Symposium and 26th Annual Student Paper Competition*, Prague, Czech Republic: American Society of Mechanical Engineers, juill. 2018, p. V005T05A013. doi: 10.1115/PVP2018-85157.
- [5] L. Ge *et al.*, « A three-dimensional progressive failure analysis of filament-wound composite pressure vessels with void defects », *Thin-Walled Struct.*, vol. 199, p. 111858, juin 2024, doi: 10.1016/j.tws.2024.111858.
- [6] A. Błachut *et al.*, « Multiscale analysis of composite pressure vessel structures wound with different fiber tensile force », *Compos. Struct.*, vol. 337, p. 118065, juin 2024, doi: 10.1016/j.compstruct.2024.118065.
- [7] D. A. McCarville, J. C. Guzman, A. K. Dillon, J. R. Jackson, et J. O. Birkland, « 3.5 Design, Manufacture and Test of Cryotank Components », in *Comprehensive Composite Materials II*, Elsevier, 2018, p. 153-179. doi: 10.1016/B978-0-12-803581-8.09958-6.
- [8] A. M. Kamal, T. A. El-Sayed, A. M. A. El-Butch, et S. H. Farghaly, « Analytical and finite element modeling of pressure vessels for seawater reverse osmosis desalination plants », *Desalination*, vol. 397, p. 126-139, nov. 2016, doi: 10.1016/j.desal.2016.06.015.
- [9] E. Lainé, J.-C. Dupré, J.-C. Grandidier, et M. Cruz, « Instrumented tests on composite pressure vessels (type IV) under internal water pressure », *Int. J. Hydrog. Energy*, vol. 46, n° 1, p. 1334-1346, janv. 2021, doi: 10.1016/j.ijhydene.2020.09.160.
- [10] M. Nebe, A. Soriano, C. Braun, P. Middendorf, et F. Walther, « Analysis on the mechanical response of composite pressure vessels during internal pressure loading: FE modeling and experimental correlation », *Compos. Part B Eng.*, vol. 212, p. 108550, mai 2021, doi: 10.1016/j.compositesb.2020.108550.
- [11] CORENSTOCK, « Life cycle oriented design & systems approach for energy efficiency of heating system storage ». [En ligne]. Disponible sur: <https://corenstock.wp.imt.fr/>
- [12] M. Azeem, H. Haji Ya, M. Azad Alam, M. Kumar, et P. Stabla, « Application of Filament Winding Technology in Composite Pressure Vessels and Challenges: A Review », *J. Energy Storage*, p. 22, 2022.
- [13] H. Jesrani, « Making It — Chapter 4: (Thin & Hollow) Filament Winding », Medium. [En ligne]. Disponible sur: <https://medium.com/@hpjesrani/filament-winding-94c796ca28f0>
- [14] P. Krawczak, « Réservoirs haute pression en composites », *Plast. Compos.*, août 2015, doi: 10.51257/a-v1-am5530.
- [15] M. Ahmadi Jebeli et M. Heidari-Rarani, « Development of Abaqus WCM plugin for progressive failure analysis of type IV composite pressure vessels based on Puck failure criterion », *Eng. Fail. Anal.*, vol. 131, p. 105851, janv. 2022, doi: 10.1016/j.engfailanal.2021.105851.
- [16] A. Air, M. Shamsuddoha, et B. Gangadhara Prusty, « A review of Type V composite pressure vessels and automated fiber placement based manufacturing », *Compos. Part B Eng.*, vol. 253, p. 110573, mars 2023, doi: 10.1016/j.compositesb.2023.110573.

- [17] Q. Ma, M. R. M. Rejab, M. Azeem, S. A. Hassan, B. Yang, et A. P. Kumar, « Opportunities and challenges on composite pressure vessels (CPVs) from advanced filament winding machinery: A short communication », *Int. J. Hydrog. Energy*, vol. 57, p. 1364-1372, févr. 2024, doi: 10.1016/j.ijhydene.2024.01.133.
- [18] W. Li et G. Palardy, « Damage monitoring methods for fiber-reinforced polymer joints: A review », *Compos. Struct.*, vol. 299, p. 116043, nov. 2022, doi: 10.1016/j.compstruct.2022.116043.
- [19] O. Ahmed, X. Wang, M.-V. Tran, et M.-Z. Ismadi, « Advancements in fiber-reinforced polymer composite materials damage detection methods: Towards achieving energy-efficient SHM systems », *Compos. Part B Eng.*, vol. 223, p. 109136, oct. 2021, doi: 10.1016/j.compositesb.2021.109136.
- [20] A. Huijter, X. Zhang, C. Kassapoglou, et L. Pahlavan, « Feasibility evaluation for development of composite propellers with embedded piezoelectric sensors », *Mar. Struct.*, vol. 84, p. 103231, juill. 2022, doi: 10.1016/j.marstruc.2022.103231.
- [21] S. Mohanta, Y. Padarthy, S. Chokkapu, J. Gupta, et S. Neogi, « Ultra-violet health monitoring of smart composite laminate using embedded fiber Bragg grating sensors », *J. Compos. Mater.*, vol. 54, n° 22, p. 3143-3158, sept. 2020, doi: 10.1177/0021998320911709.
- [22] T. Feng *et al.*, « Real-time self-monitoring and smart bend recognizing of fiber-reinforced polymer composites enabled by embedded magnetic fibers », *Compos. Sci. Technol.*, vol. 232, p. 109869, févr. 2023, doi: 10.1016/j.compscitech.2022.109869.
- [23] B.-H. Choi et I.-B. Kwon, « Damage mapping using strain distribution of an optical fiber embedded in a composite cylinder after low-velocity impacts », *Compos. Part B Eng.*, vol. 173, p. 107009, sept. 2019, doi: 10.1016/j.compositesb.2019.107009.
- [24] R. K. Langat, E. De Luycker, A. Cantarel, et M. Rakotondrabe, « Toward the development of a new smart composite structure based on piezoelectric polymer and flax fiber materials: Manufacturing and experimental characterization », *Mech. Adv. Mater. Struct.*, p. 1-15, oct. 2023, doi: 10.1080/15376494.2023.2271746.
- [25] M. C. Koecher, J. H. Pande, S. Merkle, S. Henderson, D. T. Fullwood, et A. E. Bowden, « Piezoresistive in-situ strain sensing of composite laminate structures », *Compos. Part B Eng.*, vol. 69, p. 534-541, févr. 2015, doi: 10.1016/j.compositesb.2014.09.029.
- [26] O. Okolie, J. Latto, N. Faisal, H. Jamieson, A. Mukherji, et J. Njuguna, « Advances in structural analysis and process monitoring of thermoplastic composite pipes », *Heliyon*, vol. 9, n° 7, p. e17918, juill. 2023, doi: 10.1016/j.heliyon.2023.e17918.
- [27] C. Andreades, P. Mahmoodi, et F. Ciampa, « Characterisation of smart CFRP composites with embedded PZT transducers for nonlinear ultrasonic applications », *Compos. Struct.*, vol. 206, p. 456-466, déc. 2018, doi: 10.1016/j.compstruct.2018.08.083.
- [28] S. Lu *et al.*, « Monitoring the manufacturing process of glass fiber reinforced composites with carbon nanotube buckypaper sensor », *Polym. Test.*, vol. 52, p. 79-84, juill. 2016, doi: 10.1016/j.polymertesting.2016.04.007.
- [29] R. Min, Z. Liu, L. Pereira, C. Yang, Q. Sui, et C. Marques, « Optical fiber sensing for marine environment and marine structural health monitoring: A review », *Opt. Laser Technol.*, vol. 140, p. 107082, août 2021, doi: 10.1016/j.optlastec.2021.107082.
- [30] M. Mieloszyk, K. Majewska, et W. Ostachowicz, « Application of embedded fiber Bragg grating sensors for structural health monitoring of complex composite structures for marine applications », *Mar. Struct.*, vol. 76, p. 102903, mars 2021, doi: 10.1016/j.marstruc.2020.102903.
- [31] R. A. Silva-Muñoz et R. A. Lopez-Anido, « Structural health monitoring of marine composite structural joints using embedded fiber Bragg grating strain sensors », *Compos. Struct.*, vol. 89, n° 2, p. 224-234, juin 2009, doi: 10.1016/j.compstruct.2008.07.027.
- [32] H. Rocha, C. Semprinoschnig, et J. P. Nunes, « Sensors for process and structural health monitoring of aerospace composites: A review », *Eng. Struct.*, vol. 237, p. 112231, juin 2021, doi: 10.1016/j.engstruct.2021.112231.

- [33] R. Di Sante, « Fiber Optic Sensors for Structural Health Monitoring of Aircraft Composite Structures: Recent Advances and Applications », *Sensors*, vol. 15, n° 8, p. 18666-18713, juill. 2015, doi: 10.3390/s150818666.
- [34] A. Ghoshal, J. Ayers, M. Gurvich, M. Urban, et N. Bordick, « Experimental investigations in embedded sensing of composite components in aerospace vehicles », *Compos. Part B Eng.*, vol. 71, p. 52-62, mars 2015, doi: 10.1016/j.compositesb.2014.10.050.
- [35] P. Shrestha, Y. Park, et C.-G. Kim, « Low velocity impact localization on composite wing structure using error outlier based algorithm and FBG sensors », *Compos. Part B Eng.*, vol. 116, p. 298-312, mai 2017, doi: 10.1016/j.compositesb.2016.10.068.
- [36] M. Siahkouhi, G. Razaqpur, N. A. Hoult, M. Hajmohammadian Baghban, et G. Jing, « Utilization of carbon nanotubes (CNTs) in concrete for structural health monitoring (SHM) purposes: A review », *Constr. Build. Mater.*, vol. 309, p. 125137, nov. 2021, doi: 10.1016/j.conbuildmat.2021.125137.
- [37] K. Luo, L. Chen, et W. Liang, « Structural health monitoring of carbon fiber reinforced polymer composite laminates for offshore wind turbine blades based on dual maximum correlation coefficient method », *Renew. Energy*, vol. 201, p. 1163-1175, déc. 2022, doi: 10.1016/j.renene.2022.11.063.
- [38] D. Xu, P. F. Liu, et Z. P. Chen, « Damage mode identification and singular signal detection of composite wind turbine blade using acoustic emission », *Compos. Struct.*, vol. 255, p. 112954, janv. 2021, doi: 10.1016/j.compstruct.2020.112954.
- [39] J. Sierra-Pérez, M. A. Torres-Arredondo, et A. Güemes, « Damage and nonlinearities detection in wind turbine blades based on strain field pattern recognition. FBGs, OBR and strain gauges comparison », *Compos. Struct.*, vol. 135, p. 156-166, janv. 2016, doi: 10.1016/j.compstruct.2015.08.137.
- [40] M. L. Wymore, J. E. Van Dam, H. Ceylan, et D. Qiao, « A survey of health monitoring systems for wind turbines », *Renew. Sustain. Energy Rev.*, vol. 52, p. 976-990, déc. 2015, doi: 10.1016/j.rser.2015.07.110.
- [41] L. Zhang *et al.*, « Fatigue damage monitoring of repaired composite wind turbine blades using high-stability buckypaper sensors », *Compos. Sci. Technol.*, vol. 227, p. 109592, août 2022, doi: 10.1016/j.compscitech.2022.109592.
- [42] P. Gąsior *et al.*, « Validation of Selected Optical Methods for Assessing Polyethylene (PE) Liners Used in High Pressure Vessels for Hydrogen Storage », *Appl. Sci.*, vol. 11, n° 12, p. 5667, juin 2021, doi: 10.3390/app11125667.
- [43] E. Hugaas et A. T. Echtermeyer, « Estimating S-N curves for local fiber dominated fatigue failure in ring specimens representing filament wound pressure vessels with damage », *Compos. Part C Open Access*, vol. 5, p. 100135, juill. 2021, doi: 10.1016/j.jcomc.2021.100135.
- [44] Y. Zhao, P. Druzhinin, J. Ivens, D. Vandepitte, et S. V. Lomov, « Split-disk test with 3D Digital Image Correlation strain measurement for filament wound composites », *Compos. Struct.*, vol. 263, p. 113686, mai 2021, doi: 10.1016/j.compstruct.2021.113686.
- [45] M. Nebe, T. J. Asijee, C. Braun, J. M. J. F. van Campen, et F. Walther, « Experimental and analytical analysis on the stacking sequence of composite pressure vessels », *Compos. Struct.*, vol. 247, p. 112429, sept. 2020, doi: 10.1016/j.compstruct.2020.112429.
- [46] Y. Shao *et al.*, « High pressure strength of carbon fiber reinforced vinylester and epoxy vessels », *Compos. Struct.*, vol. 140, p. 147-156, avr. 2016, doi: 10.1016/j.compstruct.2015.12.053.
- [47] H. Y. Chou, A. P. Mouritz, M. K. Bannister, et A. R. Bunsell, « Acoustic emission analysis of composite pressure vessels under constant and cyclic pressure », *Compos. Part Appl. Sci. Manuf.*, vol. 70, p. 111-120, mars 2015, doi: 10.1016/j.compositesa.2014.11.027.
- [48] J. P. Canal, A. Micuzzi, H. Logarzo, A. Terlisky, R. Toscano, et E. Dvorkin, « On the finite element modeling of CPVs », *Comput. Struct.*, vol. 220, p. 1-13, août 2019, doi: 10.1016/j.compstruc.2019.04.007.

- [49] W. Jiang, M. Liang, M. Schiebel, S. Zaremba, et K. Drechsler, « Development of machine learning based classifier for the pressure test result prediction of type IV Composite pressure vessels », *Int. J. Hydrog. Energy*, vol. 58, p. 380-388, mars 2024, doi: 10.1016/j.ijhydene.2024.01.182.
- [50] A. M. Lepikhin, V. V. Moskvichev, et A. P. Chernyaev, « Acoustic-Emission Monitoring of the Deformation and Fracture of Metal-Composite Pressure Vessels », *J. Appl. Mech. Tech. Phys.*, vol. 59, n° 3, p. 511-518, mai 2018, doi: 10.1134/S0021894418030161.
- [51] F. Dahmene, S. Yaacoubi, M. El Mountassir, C. Langlois, et O. Bardoux, « Towards efficient acoustic emission testing of CPV, without Felicity ratio criterion, during hydrogen-filling », *Int. J. Hydrog. Energy*, vol. 41, n° 2, p. 1359-1368, janv. 2016, doi: 10.1016/j.ijhydene.2015.11.065.
- [52] Y.-J. Lee, H. Ahmed, et J.-R. Lee, « Filament-wound composite pressure vessel inspection based on rotational through-transmission laser ultrasonic propagation imaging », *Compos. Struct.*, vol. 236, p. 111871, mars 2020, doi: 10.1016/j.compstruct.2020.111871.
- [53] Q. Liu, Z. Qin, Z. Zou, Q. Lv, Y. Li, et J. Guo, « Study on inclined cracks in pressure vessels based on optical fiber ultrasonic sensors », *Opt. Fiber Technol.*, vol. 66, p. 102637, oct. 2021, doi: 10.1016/j.yofte.2021.102637.
- [54] S. Yaacoubi, P. McKeon, W. Ke, N. Declercq, et F. Dahmene, « Towards an Ultrasonic Guided Wave Procedure for Health Monitoring of Composite Vessels: Application to Hydrogen-Powered Aircraft », *Materials*, vol. 10, n° 9, p. 1097, sept. 2017, doi: 10.3390/ma10091097.
- [55] Q. Li, Z. Luo, G. Hu, et S. Zhou, « A New Probabilistic Ellipse Imaging Method Based on Adaptive Signal Truncation for Ultrasonic Guided Wave Defect Localization on Pressure Vessels », *Sensors*, vol. 22, n° 4, p. 1540, févr. 2022, doi: 10.3390/s22041540.
- [56] NF EN 4861, « Série aérospatiale — Procédure d'évaluation métrologique applicable aux mesures de champs cinématiques par corrélation d'images numériques ». décembre 2020.
- [57] NF ISO 23876, « Bouteilles à gaz — Bouteilles et tubes composites — Essai par émission acoustique (EA) pour les contrôles et les essais périodiques ». août 2022.
- [58] NF EN 15857, « Essais non destructifs Émission acoustique — Essai des polymères renforcés par des fibres ». février 2010.
- [59] NF EN ISO 16810, « Essais non destructifs — Contrôle par ultrasons — Principes généraux ». 9 mai 2014.
- [60] V. Dikshit, O. L. Seng, M. Maheshwari, et A. Asundi, « Failure assessment of aluminum liner based filament-wound hybrid riser subjected to internal hydrostatic pressure », présenté à International Conference on Experimental Mechanics 2014, C. Quan, K. Qian, A. Asundi, et F. S. Chau, Éd., Singapore, Singapore, mars 2015, p. 93021P. doi: 10.1117/12.2081041.
- [61] P. Gąsior, M. Malesa, J. Kaleta, M. Kujawińska, K. Malowany, et R. Rybczyński, « Application of complementary optical methods for strain investigation in composite high pressure vessel », *Compos. Struct.*, vol. 203, p. 718-724, nov. 2018, doi: 10.1016/j.compstruct.2018.07.060.
- [62] S. Carrino, A. Maffezzoli, et G. Scarselli, « Active SHM for composite pipes using piezoelectric sensors », *Mater. Today Proc.*, vol. 34, p. 1-9, 2021, doi: 10.1016/j.matpr.2019.12.048.
- [63] X. Qing, S. Beard, A. Kumar, H. Chan, et R. Ikegami, « Advances in the development of built-in diagnostic system for filament wound composite structures », *Compos. Sci. Technol.*, vol. 66, n° 11-12, p. 1694-1702, sept. 2006, doi: 10.1016/j.compscitech.2005.11.007.
- [64] A. Bulletti, P. Giannelli, M. Calzolari, et L. Capineri, « An Integrated Acousto/Ultrasonic Structural Health Monitoring System for Composite Pressure Vessels », *IEEE Trans. Ultrason. Ferroelectr. Freq. Control*, vol. 63, n° 6, p. 864-873, juin 2016, doi: 10.1109/TUFFC.2016.2545716.
- [65] X. Wang *et al.*, « Evaluation of embedded buckypaper sensors in composite overwrapped pressure vessels for progressive damage monitoring », *Compos. Struct.*, vol. 284, p. 115223, mars 2022, doi: 10.1016/j.compstruct.2022.115223.
- [66] L. Lin *et al.*, « Condition monitoring of composite overwrap pressure vessels based on buckypaper sensor and MXene sensor », *Compos. Commun.*, vol. 25, p. 100699, juin 2021, doi: 10.1016/j.coco.2021.100699.

- [67] W. Xiaoqiang, L. Lunyang, L. Shaowei, et L. Bohan, « Condition monitoring of composite overwrap pressure vessels using MXene sensor », *Int. J. Press. Vessels Pip.*, vol. 191, p. 104349, juin 2021, doi: 10.1016/j.ijpvp.2021.104349.
- [68] L. Zhang *et al.*, « Temperature and strain monitor of CPV by buckypaper and MXene sensor combined flexible printed circuit », *Int. J. Hydrog. Energy*, vol. 47, n° 6, p. 4211-4221, janv. 2022, doi: 10.1016/j.ijhydene.2021.10.242.
- [69] L. Zhang *et al.*, « Lifetime health monitoring of fiber reinforced composites using highly flexible and sensitive MXene/CNT film sensor », *Sens. Actuators Phys.*, vol. 332, p. 113148, déc. 2021, doi: 10.1016/j.sna.2021.113148.
- [70] Z. Liang *et al.*, « FBG-based strain monitoring and temperature compensation for composite tank », *Aerosp. Sci. Technol.*, vol. 127, p. 107724, août 2022, doi: 10.1016/j.ast.2022.107724.
- [71] I. G. Tapeinos, D. S. Zarouchas, O. K. Bergsma, S. Koussios, et R. Benedictus, « Evaluation of the mechanical performance of a composite multi-cell tank for cryogenic storage: Part I - Tank pressure window based on progressive failure analysis », *Int. J. Hydrog. Energy*, vol. 44, n° 7, p. 3917-3930, févr. 2019, doi: 10.1016/j.ijhydene.2018.12.118.
- [72] E. Saeter, K. Lasn, F. Nony, et A. T. Echtermeyer, « Embedded fiber optics for monitoring pressurization and impact of filament wound cylinders », *Compos. Struct.*, vol. 210, p. 608-617, févr. 2019, doi: 10.1016/j.compstruct.2018.11.051.
- [73] D. Munzke *et al.*, « Monitoring of type IV composite pressure vessels with multilayer fully integrated optical fiber based distributed strain sensing », *Mater. Today Proc.*, vol. 34, p. 217-223, 2021, doi: 10.1016/j.matpr.2020.02.872.
- [74] B. Glisic et D. Inaudi, « Health monitoring of a full composite CNG tanks using long-gage fiber optic sensors », *11th SPIEs Annu. Int. Symp. Smart Struct. Mater.*, vol. 5384-7, p. 10, mars 2004.
- [75] H. Rocha, P. Antunes, U. Lafont, et J. P. Nunes, « FBG SENSORS FOR PROCESS AND STRUCTURAL HEALTH MONITORING OF A SMALL TYPE III COMPOSITE PRESSURE VESSEL FOR UNMANNED AERIAL VEHICLE », présenté à Composites Meet Sustainability – Proceedings of the 20th European Conference on Composite Materials, Lausanne, Switzerland, juin 2022, p. 7.
- [76] M. Konstantaki *et al.*, « Monitoring of Torque Induced Strain in Composite Shafts with Embedded and Surface-Mounted Optical Fiber Bragg Gratings », *Sensors*, vol. 21, n° 7, p. 2403, mars 2021, doi: 10.3390/s21072403.
- [77] K. Wacharczyk *et al.*, « In-Plane Strain Measurement in Composite Structures with Fiber Bragg Grating Written in Side-Hole Elliptical Core Optical Fiber », *Materials*, vol. 15, n° 1, p. 77, déc. 2021, doi: 10.3390/ma15010077.
- [78] Z. Su et L. Ye, *Identification of damage using Lamb waves: from fundamentals to applications*. in Lecture notes in applied and computational mechanics, no. 48. Berlin: Springer, 2009.
- [79] J. Zhao, R. Wang, X. He, et W. Liu, « Strain monitoring of composite pressure vessel with thin metal liner using fiber Bragg grating », présenté à Second International Conference on Smart Materials and Nanotechnology in Engineering, J. Leng, A. K. Asundi, et W. Ecke, Éd., Weihai, China, juill. 2009, p. 74930F. doi: 10.1117/12.840654.
- [80] C. Tuloup, W. Harizi, Z. Aboura, Y. Meyer, K. Khellil, et R. Lachat, « On the use of in-situ piezoelectric sensors for the manufacturing and structural health monitoring of polymer-matrix composites: A literature review », *Compos. Struct.*, vol. 215, p. 127-149, mai 2019, doi: 10.1016/j.compstruct.2019.02.046.
- [81] S. Trigwell, E. Dervishi, et A. S. Biris, « Multifunctional carbon nanotube coatings used as strain sensors for composite tanks », *Part. Sci. Technol.*, vol. 35, n° 6, p. 674-681, nov. 2017, doi: 10.1080/02726351.2016.1194346.
- [82] D. Kinet, P. Mégret, K. Goossen, L. Qiu, D. Heider, et C. Caucheteur, « Fiber Bragg Grating Sensors toward Structural Health Monitoring in Composite Materials: Challenges and Solutions », *Sensors*, vol. 14, n° 4, p. 7394-7419, avr. 2014, doi: 10.3390/s140407394.
- [83] P. Nagulapally, M. Shamsuddoha, T. Herath, L. Djukic, et G. B. Prusty, « Mechanical and optical performance evaluations of embedded polyimide and PEEK coated distributed optical sensors in

- glass fiber reinforced composites with vinyl ester resin systems », *J. Compos. Mater.*, vol. 57, n° 10, p. 1707-1728, mai 2023, doi: 10.1177/00219983231160866.
- [84] T. Shafighfard et M. Mieloszyk, « Experimental and numerical study of the additively manufactured carbon fiber reinforced polymers including fiber Bragg grating sensors », *Compos. Struct.*, vol. 299, p. 116027, nov. 2022, doi: 10.1016/j.compstruct.2022.116027.
- [85] D. Guillon *et al.*, « Manufacturing, burst test and modeling of high pressure thermoplastic composite overwrap pressure vessel », *Compos. Struct.*, vol. 316, p. 116965, juill. 2023, doi: 10.1016/j.compstruct.2023.116965.
- [86] E. Özaslan, K. Yurdakul, et C. Talebi, « Investigation of effects of manufacturing defects on bursting behavior of composite pressure vessels with various stress ratios », *Int. J. Press. Vessels Pip.*, vol. 199, p. 104689, oct. 2022, doi: 10.1016/j.ijpvp.2022.104689.
- [87] W. T. Kim et S. S. Kim, « Design of a segment-type ring burst test device to evaluate the pressure resistance performance of composite pressure vessels », *Compos. Struct.*, vol. 242, p. 112199, juin 2020, doi: 10.1016/j.compstruct.2020.112199.
- [88] H. P. Konka, M. A. Wahab, et K. Lian, « Piezoelectric fiber composite transducers for health monitoring in composite structures », *Sens. Actuators Phys.*, vol. 194, p. 84-94, mai 2013, doi: 10.1016/j.sna.2012.12.039.
- [89] M. Ju *et al.*, « Piezoelectric Materials and Sensors for Structural Health Monitoring: Fundamental Aspects, Current Status, and Future Perspectives », *Sensors*, vol. 23, n° 1, p. 543, janv. 2023, doi: 10.3390/s23010543.
- [90] P. Jiao, K.-J. I. Egbe, Y. Xie, A. Matin Nazar, et A. H. Alavi, « Piezoelectric Sensing Techniques in Structural Health Monitoring: A State-of-the-Art Review », *Sensors*, vol. 20, n° 13, p. 3730, juill. 2020, doi: 10.3390/s20133730.
- [91] J. F. Tressler, L. Qin, et K. Uchino, « 7.21 Piezoelectric Composite Sensors », in *Comprehensive Composite Materials II*, Elsevier, 2018, p. 408-419. doi: 10.1016/B978-0-12-803581-8.03937-0.
- [92] C. Frias, H. Faria, O. Frazão, P. Vieira, et A. T. Marques, « Manufacturing and testing Composite pressure vessels with embedded sensors », *Mater. Des.*, vol. 31, n° 8, p. 4016-4022, sept. 2010, doi: 10.1016/j.matdes.2010.03.022.
- [93] M. Lin *et al.*, « Monitoring the integrity of filament-wound structures using built-in sensor networks », présenté à Smart Structures and Materials, E. H. Anderson, Éd., San Diego, CA, août 2003, p. 222. doi: 10.1117/12.483877.
- [94] W. Hufenbach, R. Böhm, M. Thieme, et T. Tyczynski, « Damage monitoring in pressure vessels and pipelines based on wireless sensor networks », *Procedia Eng.*, vol. 10, p. 340-345, 2011, doi: 10.1016/j.proeng.2011.04.058.
- [95] S. W. Park, D. H. Kang, H. J. Bang, S. O. Park, et C. G. Kim, « Strain Monitoring and Damage Detection of a Filament Wound Composite Pressure Tank Using Embedded Fiber Bragg Grating Sensors », *Key Eng. Mater.*, vol. 321-323, p. 182-185, oct. 2006, doi: 10.4028/www.scientific.net/KEM.321-323.182.
- [96] C. Hu *et al.*, « Anti-interference damage localization in Composite pressure vessels using machine learning and ultrasonic guided waves », *NDT E Int.*, vol. 140, p. 102961, déc. 2023, doi: 10.1016/j.ndteint.2023.102961.
- [97] L. Qiu, X. Deng, S. Yuan, Y. Huang, et Y. Ren, « Impact Monitoring for Aircraft Smart Composite Skins Based on a Lightweight Sensor Network and Characteristic Digital Sequences », *Sensors*, vol. 18, n° 7, p. 2218, juill. 2018, doi: 10.3390/s18072218.
- [98] Venu Gopal Madhav Annamdas et Chee Kiong Soh, « Application of Electromechanical Impedance Technique for Engineering Structures: Review and Future Issues », *J. Intell. Mater. Syst. Struct.*, vol. 21, n° 1, p. 41-59, janv. 2010, doi: 10.1177/1045389X09352816.
- [99] T. Wandowski, P. H. Malinowski, et W. M. Ostachowicz, « Temperature and damage influence on electromechanical impedance method used for carbon fiber-reinforced polymer panels », *J. Intell. Mater. Syst. Struct.*, vol. 28, n° 6, p. 782-798, avr. 2017, doi: 10.1177/1045389X16657423.

- [100] M. De Oliveira, A. Monteiro, et J. Vieira Filho, « A New Structural Health Monitoring Strategy Based on PZT Sensors and Convolutional Neural Network », *Sensors*, vol. 18, n° 9, p. 2955, sept. 2018, doi: 10.3390/s18092955.
- [101] « Acellent Technologies ». Consulté le: 19 janvier 2023. [En ligne]. Disponible sur: <https://www.acellent.com/>
- [102] M. Lin, X. Qing, A. Kumar, et S. J. Beard, « SMART Layer and SMART Suitcase for structural health monitoring applications », présenté à SPIE's 8th Annual International Symposium on Smart Structures and Materials, A.-M. R. McGowan, Éd., Newport Beach, CA, juin 2001, p. 98-106. doi: 10.1117/12.429646.
- [103] X. P. Qing, S. J. Beard, A. Kumar, T. K. Ooi, et F.-K. Chang, « Built-in Sensor Network for Structural Health Monitoring of Composite Structure », *J. Intell. Mater. Syst. Struct.*, vol. 18, n° 1, p. 39-49, janv. 2007, doi: 10.1177/1045389X06064353.
- [104] M. Lin et F.-K. Chang, « The manufacture of composite structures with a built-in network of piezoceramics », *Compos. Sci. Technol.*, vol. 62, n° 7-8, p. 919-939, juin 2002, doi: 10.1016/S0266-3538(02)00007-6.
- [105] F. Avilés, A. May-Pat, M. A. López-Manchado, R. Verdejo, A. Bachmatiuk, et M. H. Rummeli, « A comparative study on the mechanical, electrical and piezoresistive properties of polymer composites using carbon nanostructures of different topology », *Eur. Polym. J.*, vol. 99, p. 394-402, févr. 2018, doi: 10.1016/j.eurpolymj.2017.12.038.
- [106] V. Kostopoulos, A. Vavouliotis, P. Karapappas, P. Tsotra, et A. Paipetis, « Damage Monitoring of Carbon Fiber Reinforced Laminates Using Resistance Measurements. Improving Sensitivity Using Carbon Nanotube Doped Epoxy Matrix System », *J. Intell. Mater. Syst. Struct.*, vol. 20, n° 9, p. 1025-1034, juin 2009, doi: 10.1177/1045389X08099993.
- [107] T.-W. Chou, L. Gao, E. T. Thostenson, Z. Zhang, et J.-H. Byun, « An assessment of the science and technology of carbon nanotube-based fibers and composites », *Compos. Sci. Technol.*, vol. 70, n° 1, p. 1-19, janv. 2010, doi: 10.1016/j.compscitech.2009.10.004.
- [108] B. Hao et P. C. Ma, « Carbon Nanotubes for Defect Monitoring in Fiber-Reinforced Polymer Composites », in *Industrial Applications of Carbon Nanotubes*, Elsevier, 2017, p. 71-99. doi: 10.1016/B978-0-323-41481-4.00003-4.
- [109] T. Takeda, Y. Shindo, Z. Wei, Y. Kuronuma, et F. Narita, « Fatigue failure and electrical resistance behaviors of carbon nanotube-based polymer composites under uniaxial tension-tension loading in a cryogenic environment », *J. Compos. Mater.*, vol. 49, n° 4, p. 457-463, févr. 2015, doi: 10.1177/0021998314521059.
- [110] R. Moriche, M. Sánchez, A. Jiménez-Suárez, S. G. Prolongo, et A. Ureña, « Electrically conductive functionalized-GNP/epoxy based composites: From nanocomposite to multiscale glass fiber composite material », *Compos. Part B Eng.*, vol. 98, p. 49-55, août 2016, doi: 10.1016/j.compositesb.2016.04.081.
- [111] S. Lu *et al.*, « Strain sensing behaviors of GnP/epoxy sensor and health monitoring for composite materials under monotonic tensile and cyclic deformation », *Compos. Sci. Technol.*, vol. 158, p. 94-100, avr. 2018, doi: 10.1016/j.compscitech.2018.02.017.
- [112] H. Zhang, Y. Liu, M. Kuwata, E. Bilotti, et T. Peijs, « Improved fracture toughness and integrated damage sensing capability by spray coated CNTs on carbon fiber prepreg », *Compos. Part Appl. Sci. Manuf.*, vol. 70, p. 102-110, mars 2015, doi: 10.1016/j.compositesa.2014.11.029.
- [113] B. Xiao *et al.*, « In-Situ Monitoring of a Filament Wound Pressure Vessel by the MWCNT Sensor under Hydraulic Fatigue Cycling and Pressurization », *Sensors*, vol. 19, n° 6, p. 1396, mars 2019, doi: 10.3390/s19061396.
- [114] L. Zhang, X. Qu, Z. Zhao, H. Zhang, S. Lu, et X. Wang, « Health monitoring of composite pressure vessels through omnidirectional buckypaper sensor array », *Appl. Phys. A*, vol. 128, n° 3, p. 178, mars 2022, doi: 10.1007/s00339-022-05316-3.
- [115] L. Zhang *et al.*, « Damage monitoring and locating of CPV under low velocity impact using MXene sensor array », *Compos. Commun.*, vol. 34, p. 101241, oct. 2022, doi: 10.1016/j.coco.2022.101241.

- [116] S. Nauman, « Piezoresistive Sensing Approaches for Structural Health Monitoring of Polymer Composites—A Review », *Eng*, vol. 2, n° 2, p. 197-226, mai 2021, doi: 10.3390/eng2020013.
- [117] A. Lemartinel, M. Castro, O. Fouché, J.-C. De-Luca, et J.-F. Feller, « A Review of Nanocarbon-Based Solutions for the Structural Health Monitoring of Composite Parts Used in Renewable Energies », *J. Compos. Sci.*, vol. 6, n° 2, p. 32, janv. 2022, doi: 10.3390/jcs6020032.
- [118] X. Wang, B. An, S. Lu, K. Ma, L. Zhang, et T. Xu, « Electrical response of carbon nanotube buckypaper sensor subjected to monotonic tension, cycle tension and temperature », *Micro Nano Lett.*, vol. 13, n° 6, p. 862-867, juin 2018, doi: 10.1049/mnl.2017.0914.
- [119] S. Lu *et al.*, « Real-time monitoring of low-velocity impact damage for composite structures with the omnidirection carbon nanotubes' buckypaper sensors », *Struct. Health Monit.*, vol. 18, n° 2, p. 454-465, mars 2019, doi: 10.1177/1475921718757937.
- [120] L. Liu, J. Wu, et Y. Zhou, « Enhanced delamination initiation stress and monitoring sensitivity of quasi-isotropic laminates under in-plane tension by interleaving with CNT buckypaper », *Compos. Part Appl. Sci. Manuf.*, vol. 89, p. 10-17, oct. 2016, doi: 10.1016/j.compositesa.2016.03.006.
- [121] L. Zhang *et al.*, « Strain and crack growth monitoring of aluminum alloy sheet using high-sensitivity buckypaper film sensors », *Sens. Actuators Phys.*, vol. 363, p. 114697, déc. 2023, doi: 10.1016/j.sna.2023.114697.
- [122] S. Sarma, S. Singh, et A. Garg, « Laminated Ag and Ag/CNT nanocomposite films as sensing element for efficient thin film temperature sensors », *Measurement*, vol. 172, p. 108876, févr. 2021, doi: 10.1016/j.measurement.2020.108876.
- [123] M. Naguib, V. N. Mochalin, M. W. Barsoum, et Y. Gogotsi, « 25th Anniversary Article: MXenes: A New Family of Two-Dimensional Materials », *Adv. Mater.*, vol. 26, n° 7, p. 992-1005, févr. 2014, doi: 10.1002/adma.201304138.
- [124] J. Halim *et al.*, « X-ray photoelectron spectroscopy of select multi-layered transition metal carbides (MXenes) », *Appl. Surf. Sci.*, vol. 362, p. 406-417, janv. 2016, doi: 10.1016/j.apsusc.2015.11.089.
- [125] L. Zhang *et al.*, « Mechanical behavior monitoring of composite hybrid bonded-riveted joints using high-stability MXENE sensors », *Polym. Compos.*, vol. 45, n° 8, p. 7316-7328, juin 2024, doi: 10.1002/pc.28267.
- [126] Z. M. Hafizi, J. Epaarachchi, et K. T. Lau, « Impact location determination on thin laminated composite plates using an NIR-FBG sensor system », *Measurement*, vol. 61, p. 51-57, févr. 2015, doi: 10.1016/j.measurement.2014.08.040.
- [127] M. Maheshwari, V. G. M. Annamdas, J. H. L. Pang, A. Asundi, et S. C. Tjin, « Crack monitoring using multiple smart materials; fiber-optic sensors & piezo sensors », *Int. J. Smart Nano Mater.*, vol. 8, n° 1, p. 41-55, janv. 2017, doi: 10.1080/19475411.2017.1298220.
- [128] B.-W. Jang et C.-G. Kim, « Real-time detection of low-velocity impact-induced delamination onset in composite laminates for efficient management of structural health », *Compos. Part B Eng.*, vol. 123, p. 124-135, août 2017, doi: 10.1016/j.compositesb.2017.05.019.
- [129] S. Nag-Chowdhury, H. Bellegou, I. Pillin, M. Castro, P. Longrais, et J. F. Feller, « Non-intrusive health monitoring of infused composites with embedded carbon quantum piezo-resistive sensors », *Compos. Sci. Technol.*, vol. 123, p. 286-294, févr. 2016, doi: 10.1016/j.compscitech.2016.01.004.
- [130] M. Ramakrishnan, G. Rajan, Y. Semenova, et G. Farrell, « Overview of Fiber Optic Sensor Technologies for Strain/Temperature Sensing Applications in Composite Materials », *Sensors*, vol. 16, n° 1, p. 99, janv. 2016, doi: 10.3390/s16010099.
- [131] P. Gasior et J. Kaleta, « OPTICAL FIBER BASED STRUCTURAL HEALTH MONITORING FOR HIGH PRESSURE HYDROGEN VESSELS FOR STATIONARY AND AUTOMOTIVE APPLICATION », déc. 2013.
- [132] W. Blazejewski, A. Czulak, P. Gasior, J. Kaleta, et R. Mech, « SMART composite high pressure vessels with integrated optical fiber sensors », présenté à SPIE Smart Structures and Materials + Nondestructive Evaluation and Health Monitoring, M. Tomizuka, Éd., San Diego, California, USA, mars 2010, p. 764712. doi: 10.1117/12.847251.

- [133] M. Hirsch, D. Majchrowicz, P. Wierzba, M. Weber, M. Bechelany, et M. Jędrzejewska-Szczerska, « Low-Coherence Interferometric Fiber-Optic Sensors with Potential Applications as Biosensors », *Sensors*, vol. 17, n° 2, p. 261, janv. 2017, doi: 10.3390/s17020261.
- [134] D. Inaudi, « FIBER OPTIC SENSOR NETWORK FOR THE MONITORING OF CIVIL ENGINEERING STRUCTURES », ECOLE POLYTECHNIQUE FEDERALE DE LAUSANNE, Lausanne, Suisse, 1997.
- [135] L. Maurin, P. Ferdinand, F. Nony, et S. Villalonga, « OFDR Distributed Strain Measurements for SHM of Hydrostatic Stressed Structures: An Application to High Pressure Hydrogen Storage Type IV Composite Vessels - H2E Project », 2014.
- [136] S. M. Klute, D. R. Metrey, N. Garg, N. A. A. Rahim, et B. Va, « IN-SITU STRUCTURAL HEALTH MONITORING OF COMPOSITE-OVERWRAPPED PRESSURE VESSELS », 2016.
- [137] Md. Shamsuddoha, M. David, E. Oromiehie, et B. G. Prusty, « Distributed fiber optic sensor based monitoring of thermoplastic carbon composite cylinders under biaxial loading: Experimental and numerical investigations », *Compos. Struct.*, vol. 261, p. 113277, avr. 2021, doi: 10.1016/j.compstruct.2020.113277.
- [138] G. Souza et J. Tarpani, « Using OBR for pressure monitoring and BVID detection in type IV Composite pressure vessels », *J. Compos. Mater.*, vol. 55, n° 3, p. 423-436, févr. 2021, doi: 10.1177/0021998320951616.
- [139] « Home », Luna. Consulté le: 18 janvier 2023. [En ligne]. Disponible sur: <https://lunainc.com/>
- [140] J. H. L. Grave, M. L. Håheim, et A. T. Echtermeyer, « Measuring changing strain fields in composites with Distributed Fiber-Optic Sensing using the optical backscatter reflectometer », *Compos. Part B Eng.*, vol. 74, p. 138-146, juin 2015, doi: 10.1016/j.compositesb.2015.01.003.
- [141] R. Werlink et F. Pena, « NASA Prototype All Composite Tank Cryogenic Pressure Tests to Failure with Structural Health Monitoring », in *Structural Health Monitoring 2015*, Destech Publications, 2015. doi: 10.12783/SHM2015/362.
- [142] I. G. Tapeinos *et al.*, « Evaluation of the mechanical performance of a composite multi-cell tank for cryogenic storage: Part II – Experimental assessment », *Int. J. Hydrog. Energy*, vol. 44, n° 7, p. 3931-3943, févr. 2019, doi: 10.1016/j.ijhydene.2018.12.063.
- [143] Y. C. Chen, C. C. Hsieh, et C. C. Lin, « Strain measurement for composite tubes using embedded, fiber Bragg grating sensor », *Sens. Actuators Phys.*, vol. 167, n° 1, p. 63-69, mai 2011, doi: 10.1016/j.sna.2011.02.035.
- [144] D. H. Kang, C. U. Kim, et C. G. Kim, « The embedment of fiber Bragg grating sensors into filament wound pressure tanks considering multiplexing », *NDT E Int.*, vol. 39, n° 2, p. 109-116, mars 2006, doi: 10.1016/j.ndteint.2005.07.013.
- [145] J. Hao, J. Leng, et Z. Wei, « Non-destructive Evaluation of Composite Pressure Vessel by Using FBG Sensors », *Chin. J. Aeronaut.*, vol. 20, n° 2, p. 120-123, avr. 2007, doi: 10.1016/S1000-9361(07)60017-X.
- [146] Y. Kuang, Y. Guo, L. Xiong, et W. Liu, « Packaging and Temperature Compensation of Fiber Bragg Grating for Strain Sensing: A Survey », *Photonic Sens.*, vol. 8, n° 4, p. 320-331, déc. 2018, doi: 10.1007/s13320-018-0504-y.
- [147] W. Zhou *et al.*, « Review on optimization design, failure analysis and non-destructive testing of composite hydrogen storage vessel », *Int. J. Hydrog. Energy*, p. S0360319922041052, sept. 2022, doi: 10.1016/j.ijhydene.2022.09.028.
- [148] J. S. Chilles, A. F. Koutsomitopoulou, A. J. Croxford, et I. P. Bond, « Monitoring cure and detecting damage in composites with inductively coupled embedded sensors », *Compos. Sci. Technol.*, vol. 134, p. 81-88, oct. 2016, doi: 10.1016/j.compscitech.2016.07.028.
- [149] S. M. A. Musa, M. H. Dzulkifli, A. I. Azmi, et S. A. Ibrahim, « Embedded and Surface-Mounted Fiber Bragg Grating as a Multiparameter Sensor in Fiber-Reinforced Polymer Composite Materials: A Review », *IEEE Access*, vol. 11, p. 86611-86644, 2023, doi: 10.1109/ACCESS.2023.3304679.
- [150] I. Kressel *et al.*, « Flight validation of an embedded structural health monitoring system for an unmanned aerial vehicle », *Smart Mater. Struct.*, vol. 24, n° 7, p. 075022, juill. 2015, doi: 10.1088/0964-1726/24/7/075022.

- [151] D. A. Krohn, *Fiber optic sensors: fundamentals and applications*, Fourth edition. Bellingham, Washington, USA: SPIE Press, 2014.
- [152] R. Janeliukstis et D. Mironovs, « Smart Composite Structures with Embedded Sensors for Load and Damage Monitoring – A Review », *Mech. Compos. Mater.*, vol. 57, n° 2, p. 131-152, mai 2021, doi: 10.1007/s11029-021-09941-6.
- [153] H. Mahmood, A. Dorigato, et A. Pegoretti, « Temperature Dependent Strain/Damage Monitoring of Glass/Epoxy Composites with Graphene as a Piezoresistive Interphase », *Fibers*, vol. 7, n° 2, p. 17, févr. 2019, doi: 10.3390/fib7020017.
- [154] V. Birman, « Thermal effects on measurements of dynamic processes in composite structures using piezoelectric sensors », *Smart Mater. Struct.*, vol. 5, n° 4, p. 379-385, août 1996, doi: 10.1088/0964-1726/5/4/001.
- [155] F. Ren, I. N. Giannakeas, Z. Sharif Khodaei, et M. H. F. Aliabadi, « The temperature effects on embedded PZT signals in structural health monitoring for composite structures with different thicknesses », *NDT E Int.*, vol. 141, p. 102988, janv. 2024, doi: 10.1016/j.ndteint.2023.102988.
- [156] V. Memmolo, L. Maio, et F. Ricci, « Assessment of Damage in Composite Pressure Vessels Using Guided Waves », *Sensors*, vol. 22, n° 14, p. 5182, juill. 2022, doi: 10.3390/s22145182.
- [157] X. Qu *et al.*, « Various static loading condition monitoring of carbon fiber composite cylinder with integrated optical fiber sensors », *Opt. Fiber Technol.*, vol. 83, p. 103685, mars 2024, doi: 10.1016/j.yofte.2024.103685.
- [158] T. M. J. Gebhart, M. Seeberg, H. Çelik, R. Dahlmann, et C. Hopmann, « Advanced methods for the detection of measurement outliers in fiber optic strain measurements for non-destructive monitoring of the structural health of composite over-wrapped pressure vessels of type-IV », *Measurement*, vol. 226, p. 114133, févr. 2024, doi: 10.1016/j.measurement.2024.114133.
- [159] P. M. Ferreira, M. A. Machado, M. S. Carvalho, et C. Vidal, « Embedded Sensors for Structural Health Monitoring: Methodologies and Applications Review », *Sensors*, vol. 22, n° 21, p. 8320, oct. 2022, doi: 10.3390/s22218320.
- [160] H. Montazerian, A. Rashidi, A. S. Milani, et M. Hoorfar, « Integrated Sensors in Advanced Composites: A Critical Review », *Crit. Rev. Solid State Mater. Sci.*, vol. 45, n° 3, p. 187-238, mai 2020, doi: 10.1080/10408436.2019.1588705.
- [161] S. C. Her, B. R. Yao, S. C. Lan, et C. Y. Liu, « Stress Analysis of a Resin Pocket Embedded in Laminated Composites for an Optical Fiber Sensor », *Key Eng. Mater.*, vol. 419-420, p. 293-296, oct. 2009, doi: 10.4028/www.scientific.net/KEM.419-420.293.
- [162] A. Al-Shawk, H. Tanabi, et B. Sabuncuoglu, « Investigation of stress distributions in the resin rich region and failure behavior in glass fiber composites with microvascular channels under tensile loading », *Compos. Struct.*, vol. 192, p. 101-114, mai 2018, doi: 10.1016/j.compstruct.2018.02.061.
- [163] A. T. T. Nguyen et A. C. Orifici, « Structural assessment of microvascular self-healing laminates using progressive damage finite element analysis », *Compos. Part Appl. Sci. Manuf.*, vol. 43, n° 11, p. 1886-1894, nov. 2012, doi: 10.1016/j.compositesa.2012.06.005.
- [164] N. Lammens, G. Luyckx, E. Voet, W. Van Paepegem, et J. Degrieck, « Finite element prediction of resin pocket geometry around embedded optical fiber sensors in prepreg composites », *Compos. Struct.*, vol. 132, p. 825-832, nov. 2015, doi: 10.1016/j.compstruct.2015.07.003.
- [165] S. Masmoudi, A. El Mahi, et S. Turki, « Use of piezoelectric as acoustic emission sensor for in situ monitoring of composite structures », *Compos. Part B Eng.*, vol. 80, p. 307-320, oct. 2015, doi: 10.1016/j.compositesb.2015.06.003.
- [166] K. Ha, « A COMBINED PIEZOELECTRIC COMPOSITE ACTUATOR AND ITS APPLICATION TO WING/BLADE TIPS », Georgia Institute of Technology, Georgia, 2005.
- [167] C. A. Paget et K. Levin, « Structural integrity of composites with embedded piezoelectric ceramic transducers », présenté à 1999 Symposium on Smart Structures and Materials, N. M. Wereley, Éd., Newport Beach, CA, juin 1999, p. 306-313. doi: 10.1117/12.350710.

- [168] D. J. Warkentin, E. F. Crawley, et S. D. Senturia, « The Feasibility of Embedded Electronics for Intelligent Structures », *J. Intell. Mater. Syst. Struct.*, vol. 3, n° 3, p. 462-482, juill. 1992, doi: 10.1177/1045389X9200300305.
- [169] S. Mall et J. M. Coleman, « Monotonic and fatigue loading behavior of quasi-isotropic graphite/epoxy laminate embedded with piezoelectric sensor », *Smart Mater. Struct.*, vol. 7, n° 6, p. 822-832, déc. 1998, doi: 10.1088/0964-1726/7/6/010.
- [170] Y. Huang, F. Ghezzi, et S. Nemat-Nasser, « Onset of Resin Micro-cracks in Unidirectional Glass Fiber Laminates with Integrated SHM Sensors: Numerical Analysis », *Struct. Health Monit.*, vol. 8, n° 6, p. 493-507, nov. 2009, doi: 10.1177/1475921709340979.
- [171] H. P. Konka, M. A. Wahab, et K. Lian, « The effects of embedded piezoelectric fiber composite sensors on the structural integrity of glass-fiber–epoxy composite laminate », *Smart Mater. Struct.*, vol. 21, n° 1, p. 015016, janv. 2012, doi: 10.1088/0964-1726/21/1/015016.
- [172] N. Lammens, G. Luyckx, W. Van Paeppegem, et J. Degrieck, « Finite element prediction of resin pocket geometries around arbitrary inclusions in composites: Case study for an embedded optical fiber interrogator », *Compos. Struct.*, vol. 146, p. 95-107, juin 2016, doi: 10.1016/j.compstruct.2016.03.001.
- [173] Y. Xiao, W. Qiao, H. Fukuda, et H. Hatta, « The effect of embedded devices on structural integrity of composite laminates », *Compos. Struct.*, vol. 153, p. 21-29, oct. 2016, doi: 10.1016/j.compstruct.2016.06.007.
- [174] M. Javdanitehran, R. Hoffmann, J. Groh, M. Vossiek, et G. Ziegmann, « Effect of embedded printed circuit board (PCB) sensors on the mechanical behavior of glass fiber-reinforced polymer (GFRP) structures », *Smart Mater. Struct.*, vol. 25, n° 6, p. 065016, juin 2016, doi: 10.1088/0964-1726/25/6/065016.
- [175] X. Chen *et al.*, « Embedding stretchable, mesh-structured piezoresistive sensor for in-situ damage detection of glass fiber-reinforced composite », *Compos. Sci. Technol.*, vol. 233, p. 109926, mars 2023, doi: 10.1016/j.compscitech.2023.109926.
- [176] X. W. Ye, Y. H. Su, et J. P. Han, « Structural Health Monitoring of Civil Infrastructure Using Optical Fiber Sensing Technology: A Comprehensive Review », *Sci. World J.*, vol. 2014, p. 1-11, 2014, doi: 10.1155/2014/652329.
- [177] D. C. Lee, J. J. Lee, et S. J. Yun, « The mechanical characteristics of smart composite structures with embedded optical fiber sensors », *Compos. Struct.*, vol. 32, n° 1-4, p. 39-50, janv. 1995, doi: 10.1016/0263-8223(95)00038-0.
- [178] W. Ostachowicz et J. A. Güemes, Éd., *New Trends in Structural Health Monitoring*, vol. 542. in CISM International Centre for Mechanical Sciences, vol. 542. Vienna: Springer Vienna, 2013. doi: 10.1007/978-3-7091-1390-5.
- [179] D. J. Hartl, G. J. Frank, et J. W. Baur, « Effects of microchannels on the mechanical performance of multifunctional composite laminates with unidirectional laminae », *Compos. Struct.*, vol. 143, p. 242-254, mai 2016, doi: 10.1016/j.compstruct.2016.01.106.
- [180] K. Shivakumar et A. Bhargava, « Failure Mechanics of a Composite Laminate Embedded with a Fiber Optic Sensor », *J. Compos. Mater.*, vol. 39, n° 9, p. 777-798, mai 2005, doi: 10.1177/0021998305048156.
- [181] K. Shivakumar et L. Emmanwori, « Mechanics of Failure of Composite Laminates with an Embedded Fiber Optic Sensor », *J. Compos. Mater.*, vol. 38, n° 8, p. 669-680, avr. 2004, doi: 10.1177/0021998304042393.
- [182] A. Y. Fedorov, N. A. Kosheleva, V. P. Matveenko, et G. S. Serovaev, « Strain measurement and stress analysis in the vicinity of a fiber Bragg grating sensor embedded in a composite material », *Compos. Struct.*, vol. 239, p. 111844, mai 2020, doi: 10.1016/j.compstruct.2019.111844.
- [183] Y. Ma, C. Xiaoquan, J. Zhang, D. Zhao, et W. Huang, « Prediction of resin pocket geometry around rigid fiber inclusion in composite laminate by hot-pressing of prepregs », *J. Compos. Mater.*, vol. 54, n° 15, p. 1987-1999, juin 2020, doi: 10.1177/0021998319889399.
- [184] Luna OBR 4600, [En ligne]. Disponible sur: https://lunainc.com/sites/default/files/assets/files/data-sheets/OBR4600_DS_REV6_111623.pdf

- [185] S.-C. Her et W.-C. Hsu, « Strain and Temperature Sensitivities Along with Mechanical Properties of CNT Buckypaper Sensors », *Sensors*, vol. 20, n° 11, p. 3067, mai 2020, doi: 10.3390/s20113067.
- [186] « Piezoelectric Sensor », Components101. Consulté le: 19 janvier 2023. [En ligne]. Disponible sur: <https://components101.com/sensors/piezoelectric-sensor>
- [187] A. J. Brunner, « A Review of Approaches for Mitigating Effects from Variable Operational Environments on Piezoelectric Transducers for Long-Term Structural Health Monitoring », *Sensors*, vol. 23, n° 18, p. 7979, sept. 2023, doi: 10.3390/s23187979.
- [188] N. Gariya, S. Kumar, A. Shaikh, B. Prasad, et H. Nautiyal, « A review on soft pneumatic actuators with integrated or embedded soft sensors », *Sens. Actuators Phys.*, vol. 372, p. 115364, juill. 2024, doi: 10.1016/j.sna.2024.115364.
- [189] L. Yuan *et al.*, « Piezoelectric PAN/BaTiO₃ nanofiber membranes sensor for structural health monitoring of real-time damage detection in composite », *Compos. Commun.*, vol. 25, p. 100680, juin 2021, doi: 10.1016/j.coco.2021.100680.
- [190] T. M. Brugo *et al.*, « Self-sensing hybrid composite laminate by piezoelectric nanofibers interleaving », *Compos. Part B Eng.*, vol. 212, p. 108673, mai 2021, doi: 10.1016/j.compositesb.2021.108673.
- [191] Y. Su *et al.*, « An implantable, compatible and networkable nanocomposite piezoresistive sensor for in situ acquisition of dynamic responses of CFRPs », *Compos. Sci. Technol.*, vol. 208, p. 108747, mai 2021, doi: 10.1016/j.compscitech.2021.108747.
- [192] X. Hu, G. Zhang, X. Liu, K. Chen, et X. Zhang, « Design of High-Sensitivity Flexible Low-Profile Spiral Antenna Sensor for GIS Built-in PD Detection », *Sensors*, vol. 23, n° 10, p. 4722, mai 2023, doi: 10.3390/s23104722.
- [193] J. DeGraff *et al.*, « Scalable and passive carbon nanotube thin-film sensor for detecting micro-strains and potential impact damage in fiber-reinforced composite materials », *Nanocomposites*, vol. 9, n° 1, p. 215-230, déc. 2023, doi: 10.1080/20550324.2023.2291625.
- [194] P. Kowol, S. Bargmann, P. Görrn, et J. Wilmers, « Strain relief by controlled cracking in highly stretchable multi-layer composites », *Extreme Mech. Lett.*, vol. 54, p. 101724, juill. 2022, doi: 10.1016/j.eml.2022.101724.
- [195] M. Nachtane *et al.*, « An Overview of the Recent Advances in Composite Materials and Artificial Intelligence for Hydrogen Storage Vessels Design », *J. Compos. Sci.*, vol. 7, n° 3, p. 119, mars 2023, doi: 10.3390/jcs7030119.
- [196] J.-M. Lee, Y. Choi, et J.-R. Lee, « Laser structural training, artificial intelligence-based acoustic emission localization and structural/noise signal distinguishment in a thick FCEV fuel tank », *Int. J. Hydrog. Energy*, vol. 47, n° 6, p. 4236-4254, janv. 2022, doi: 10.1016/j.ijhydene.2021.10.262.
- [197] Q. Wang *et al.*, « Failure prediction and optimization for composite pressure vessel combining FEM simulation and machine learning approach », *Compos. Struct.*, vol. 337, p. 118099, juin 2024, doi: 10.1016/j.compstruct.2024.118099.
- [198] M. Lenner, A. Frank, L. Yang, T. M. Roininen, et K. Bohnert, « Long-Term Reliability of Fiber-Optic Current Sensors », *IEEE Sens. J.*, vol. 20, n° 2, p. 823-832, janv. 2020, doi: 10.1109/JSEN.2019.2944346.
- [199] A. Maslo, M. Hodzic, E. Skaljo, et A. Mujcic, « Aging and Degradation of Optical Fiber Parameters in a 16-Year-Long Period of Usage », *Fiber Integr. Opt.*, vol. 39, n° 1, p. 39-52, janv. 2020, doi: 10.1080/01468030.2020.1725185.
- [200] « THE IMPACT OF WATER ON FIBER OPTIC CABLE », *Datwyler Datwyler Cabling Solution*, Germany, 2014.
- [201] S. G. Glaesmann, « Optical Fiber Mechanical Reliability, Review of Research at Corning Optical Strength Laboratory », *Corning WP*, juill. 2017.
- [202] Y. Chen et K. Lewis, « Thermal Agng Impact on Optical Fiber with Corning CPC Coating », *Corning*, New York USA, 2014.

- [203] J. N. Eiras, L. Gavérina, et J.-M. Roche, « Durability Assessment of Bonded Piezoelectric Wafer Active Sensors for Aircraft Health Monitoring Applications », *Sensors*, vol. 24, n° 2, p. 450, janv. 2024, doi: 10.3390/s24020450.
- [204] X. Liu, Y. Xu, X. Wang, Y. Ran, et W. Zhang, « Effect of Adhesive and Its Aging on the Performance of Piezoelectric Sensors in Structural Health Monitoring Systems », *Metals*, vol. 10, n° 10, p. 1342, oct. 2020, doi: 10.3390/met10101342.
- [205] R. P. Dahl-Hansen *et al.*, « On the Effect of Water-Induced Degradation of Thin-Film Piezoelectric Microelectromechanical Systems », *J. Microelectromechanical Syst.*, vol. 30, n° 1, p. 105-115, févr. 2021, doi: 10.1109/JMEMS.2020.3031201.
- [206] A. Del Bosque, X. F. Sánchez-Romate, D. Calvo, M. Sánchez, et A. Ureña, « Mechanical and sensing performance under hydrothermal ageing of wearable sensors made of polydimethylsiloxane with graphitic nanofillers », *Polym. Degrad. Stab.*, vol. 209, p. 110278, mars 2023, doi: 10.1016/j.polymdegradstab.2023.110278.
- [207] G. Murali, J. K. R. Modigunta, Y. H. Park, S. Y. Park, et I. In, « Stability and Degradation of MXene », in *Fundamental Aspects and Perspectives of MXenes*, M. Khalid, A. N. Grace, A. Arulraj, et A. Numan, Éd., in *Engineering Materials.*, Cham: Springer International Publishing, 2022, p. 87-107. doi: 10.1007/978-3-031-05006-0_5.
- [208] « Design oriented life cycle & systemic approach for energy efficiency of heating system storage ». [En ligne]. Disponible sur: <https://corenstock.wp.imt.fr/>